



King's Research Portal

DOI:

[10.1038/mp.2017.44](https://doi.org/10.1038/mp.2017.44)

Document Version

Peer reviewed version

[Link to publication record in King's Research Portal](#)

Citation for published version (APA):

Culverhouse, R. C., Saccone, N. L., Horton, A. C., Anstey, K. J., Banaschewski, T., Burmeister, M., Cohen-Woods, S., Etain, B., Fisher, H. L., Goldman, N., Guillaume, S., Horwood, J., Juhasz, G., Lester, K. J., Mandelli, L., Middeldorp, C. M., Olié, E., Villafuerte, S., Air, T. M., ... Bierut, L. J. (2018). Collaborative meta-analysis finds no evidence of a strong interaction between stress and 5-HTTLPR genotype contributing to the development of depression. *Molecular Psychiatry*, 23(1), 133-142. <https://doi.org/10.1038/mp.2017.44>

Citing this paper

Please note that where the full-text provided on King's Research Portal is the Author Accepted Manuscript or Post-Print version this may differ from the final Published version. If citing, it is advised that you check and use the publisher's definitive version for pagination, volume/issue, and date of publication details. And where the final published version is provided on the Research Portal, if citing you are again advised to check the publisher's website for any subsequent corrections.

General rights

Copyright and moral rights for the publications made accessible in the Research Portal are retained by the authors and/or other copyright owners and it is a condition of accessing publications that users recognize and abide by the legal requirements associated with these rights.

- Users may download and print one copy of any publication from the Research Portal for the purpose of private study or research.
- You may not further distribute the material or use it for any profit-making activity or commercial gain
- You may freely distribute the URL identifying the publication in the Research Portal

Take down policy

If you believe that this document breaches copyright please contact librarypure@kcl.ac.uk providing details, and we will remove access to the work immediately and investigate your claim.

1
2
3
4
5
6
7
8
9
10
11
12
13
14
15
16
17
18
19
20
21
22
23
24
25
26
27
28
29
30
31
32
33
34

Candidalysin is a fungal peptide toxin critical for mucosal infection

David L. Moyes^{1*}, Duncan Wilson^{2*†}, Jonathan P. Richardson^{1*}, Selene Mogavero^{2*}, Shirley X. Tang¹, Julia Wernecke^{3,4}, Sarah Höfs², Remi L. Gratacap⁵, Jon Robbins⁶, Manohursingh Runglall^{1#}, Celia Murciano^{1##}, Mariana Blagojevic¹, Selvam Thavaraj¹, Toni M. Förster², Betty Hebecker^{2,7}, Lydia Kasper², Gema Vizcay⁸, Simona I. Iancu¹, Nessim Kichik^{1,9}, Antje Häder¹⁰, Oliver Kurzai¹⁰, Ting Luo¹¹, Thomas Krüger¹¹, Olaf Kniemeyer¹¹, Ernesto Cota⁹, Oliver Bader¹², Robert T. Wheeler⁵, Thomas Gutschmann³, Bernhard Hube^{2,13,14} and Julian R. Naglik¹

- ¹ Mucosal & Salivary Biology Division, Dental Institute, King's College London, UK
- ² Department of Microbial Pathogenicity Mechanisms, Hans Knöll Institute, Jena, Germany
- ³ Research Center Borstel, Division of Biophysics, Borstel, Germany
- ⁴ Deutsches Elektronen-Synchrotron DESY, Hamburg, Germany
- ⁵ Department of Molecular & Biomedical Sciences, University of Maine, Orono, ME, USA
- ⁶ Wolfson CARD, King's College, Guy's Campus, London, UK
- ⁷ Research Group Microbial Immunology, Hans Knöll Institute, Jena, Germany
- ⁸ Centre for Ultrastructural Imaging, King's College London, UK
- ⁹ Department of Life Sciences, Imperial College London, London, UK
- ¹⁰ Septomics Research Center, Hans-Knöll Institute and Friedrich Schiller University, Jena
- ¹¹ Department of Molecular and Applied Microbiology, Hans Knöll Institute, Jena, Germany
- ¹² Institute for Medical Microbiology, University Medical Center Göttingen, Göttingen, Germany
- ¹³ Friedrich Schiller University, Jena, Germany
- ¹⁴ Integrated Research and Treatment Center, Center for Sepsis Control and Care, Jena, Germany

* These authors contributed equally to this work.

Current address:

- † Aberdeen Fungal Group, School of Medicine, Medical Sciences and Nutrition, University of Aberdeen, Aberdeen, UK
- # NIHR Biomedical Research Centre, Guy's and St Thomas' NHS Foundation Trust, London, UK

35 # ERI Biocmed & Microbiology and Ecology Department, University of Valencia,
36 Valencia, Spain

37 **Abstract**

38 Cytolytic proteins and peptide toxins are classical virulence factors of several bacterial
39 pathogens which disrupt epithelial barrier function, damage cells and activate or modulate
40 host immune responses. Until now human pathogenic fungi were not known to possess such
41 toxins. Here we identify the first fungal cytolitic peptide toxin in the opportunistic pathogen
42 *Candida albicans*. This secreted toxin directly damages epithelial membranes, triggers a
43 danger response signalling pathway and activates epithelial immunity. Toxin-mediated
44 membrane permeabilization is enhanced by a positively charged C-terminus and triggers an
45 inward current concomitant with calcium influx. *C. albicans* strains lacking this toxin do not
46 activate or damage epithelial cells and are avirulent in animal models of mucosal infection.
47 We propose the name ‘Candidalysin’ for this cytolitic peptide toxin; a newly identified,
48 critical molecular determinant of epithelial damage and host recognition of the clinically
49 important fungus, *C. albicans*.

50

51

52 **Introduction**

53 The ability of mucosal surfaces to discriminate between commensal and pathogenic microbes
54 is essential to human health. The fungus *Candida albicans* is normally a benign member of
55 the human microbiota but is also responsible for millions of mucosal infections each year in
56 immunocompromised hosts, often with severe morbidity¹. A defining feature of *C. albicans*
57 pathogenesis is the transition from yeast to invasive filamentous hyphae². Hyphae damage
58 mucosal epithelia and induce activation of the activating protein-1 (AP-1) transcription factor
59 c-Fos (via p38-MAPK) and the MAPK phosphatase MKP1 (via ERK1/2-MAPK), which
60 trigger pro-inflammatory cytokine responses³⁻⁷. These signaling events constitute a ‘danger
61 response’ against invasive hyphae, thus serving as a sensor of pathogenic *C. albicans*
62 invasion⁸⁻¹⁴. However, it is unclear how *C. albicans* hyphae induce epithelial inflammatory
63 responses and cell damage during mucosal infections. Here we identify and characterize
64 Candidalysin, the first cytolitic peptide toxin isolated from any human fungal pathogen, as
65 the hyphal factor critical for epithelial immune activation and *C. albicans* mucosal infection.

66

67 **Ecelp is critical for epithelial activation and damage**

68 Despite the well-known association between filamentation and virulence, the molecular
69 mechanism underlying hypha-driven epithelial activation and mucosal damage has remained
70 obscure. To elucidate this mechanism, we screened a panel of *C. albicans* gene deletion

71 mutants that targeted key processes, pathways and proteins known or predicted to be
72 associated with the yeast-hyphal transition and pathogenicity (62 strains). Only hypha-
73 producing strains induced MKP1 phosphorylation (p-MKP1), c-Fos, cytokines (IL-1 α , IL-6,
74 G-CSF) and damage in oral epithelial cells (Extended Data Table 1). However, one *C.*
75 *albicans* mutant (*ece1* Δ/Δ)¹⁵ formed normal hyphae but was incapable of inducing these
76 epithelial danger responses. *C. albicans ECE1* (extent of cell elongation) is highly expressed
77 by hyphae during epithelial infection (Extended Data Fig. 1a, b) and is predicted to encode a
78 secreted protein¹⁶. To probe its function we generated a panel of *C. albicans ECE1*-mutants
79 (Extended Data Table 2). The *ece1* Δ/Δ strain formed normal hyphae on (Extended Data Fig.
80 1c), and adhered to and invaded human epithelial cells similarly to wild type *C. albicans*
81 (Extended Data Fig. 1d, e). Indeed, *ece1* Δ/Δ was capable of extensive epithelial invasion,
82 penetrating through multiple epithelial cells (Extended Data Fig. 1f). Despite this, invasive
83 *ece1* Δ/Δ hyphae did not damage epithelia or induce p-MKP1/c-Fos mediated danger
84 responses or cytokine secretion (Fig. 1a-d). Thus, Ece1p is critical for epithelial damage and
85 innate recognition of *C. albicans* hyphae *in vitro*.

86

87 **Ece1p is critical for mucosal pathogenesis**

88 We next assessed the role of *ECE1* in two *in vivo* models of *C. albicans* mucosal infection. In
89 murine oropharyngeal candidiasis (OPC)¹⁷, mice infected with *C. albicans* wild type or *ECE1*
90 re-integrand (*ece1* Δ/Δ +*ECE1*) strains exhibited disease symptoms, including extensive hyphal
91 invasion of the tongue epithelium, micro-abscesses of infiltrating neutrophils and tissue
92 damage (Fig. 1e, f, h, i). In contrast, tongue tissue from *ece1* Δ/Δ -infected animals (n =
93 17/20) showed no invasive fungi and no inflammatory infiltrates or damage (Fig. 1g). We
94 detected very low numbers of *ece1* Δ/Δ cells in only 3/20 mice (Extended Data Fig. 2a),
95 which showed no evidence of local epithelial damage (not shown). Quantification of
96 histology sections indicated that the percentage of epithelial surface infected was
97 significantly greater with the wild type and *ECE1* re-integrand strains (Extended Data Fig.
98 2b). In a zebrafish swimbladder model of mucosal infection^{18,19}, neutrophil recruitment and
99 tissue damage were both significantly lower following *ece1* Δ/Δ infection as compared with
100 the wild type strain (Fig. 1j, k, Extended Data Fig. 2c, d). Therefore, *C. albicans* Ece1p is
101 critical for mucosal pathogenesis and is an innate immune activator *in vivo*.

102

103 **Ece1p encodes a cytolytic peptide toxin**

104 Ece1p is an *in vitro* substrate for Kex2p, a Golgi-located protease that cleaves proteins after
105 lysine-arginine (KR) motifs²⁰. Ece1p contains seven KR-processing sites, suggesting it has
106 the potential to produce eight secreted peptides from *C. albicans*²⁰ (Extended Data Fig. 3a, b).
107 Liquid chromatography – tandem mass spectrometry (LC-MS/MS) analysis confirmed that
108 recombinant Kex2p (rKex2p) processes recombinant Ece1p (rEce1p) and that all eight
109 peptides generated terminated in KR (and fragments thereof, showing that less efficient
110 processing occurs also after a single K or R) (Supplementary information). The importance
111 of Kex2p-mediated Ece1p processing was demonstrated using a *kex2Δ/Δ* null strain²¹, which
112 was unable to damage oral epithelia or induce p-MKP1/c-Fos mediated danger responses or
113 cytokine secretion (Extended Data Table 1). To determine which Ece1p peptide(s) were
114 responsible for epithelial activation and damage, oral epithelial cells were incubated with
115 peptides Ece1-I-VIII (1.5 – 70 μM). Only Ece1-III₆₂₋₉₃ induced p-MKP1, c-Fos, cytokines
116 and damage (Fig. 2a-c, Extended Data Fig. 3c-e). Notably, low Ece1-III₆₂₋₉₃ concentrations
117 (1.5 – 15 μM) were sufficient to induce c-Fos DNA binding (Fig. 2d), G-CSF and GM-CSF
118 (Fig. 2c, Extended Data Fig. 3c), while high Ece1-III₆₂₋₉₃ concentrations (70 μM) were
119 required to induce damage (Fig. 2e) and the damage-associated cytokines IL-1α and IL-6,
120 respectively (Extended Data Fig. 3d, e). Ece1-III₆₂₋₉₃ could also directly lyse multiple human
121 epithelial cell types and induce hemolysis of red blood cells, a classical test for cytotoxin
122 activity (not shown). Neither the N-terminal hydrophobic region (Ece1-III₆₂₋₈₅) nor the C-
123 terminal hydrophilic region (Ece1-III₈₆₋₉₃) induced p-MKP1, c-Fos, cytokines or damage of
124 epithelial cells, either individually or in combination (Extended Data Fig. 3f-h),
125 demonstrating that the peptide containing both regions is required for activity. Therefore,
126 Ece1-III₆₂₋₉₃ is the active region of Ece1p, acting as an epithelial immune activator and a
127 cytolytic agent.

128 To confirm that Ece1-III₆₂₋₉₃ drives epithelial activation and fungal pathogenicity, we
129 generated a *C. albicans* strain lacking only the Ece1-III₆₂₋₉₃ region (*ece1Δ/Δ+ECE1_{Δ184-279}*).
130 LC-MS/MS analysis showed that the modified protein in this strain is stable, secreted, and
131 processed into each of the predicted peptide fragments, with the exception of the deleted
132 peptide toxin (Supplementary information). Like *ece1Δ/Δ*, *ece1Δ/Δ+ECE1_{Δ184-279}* efficiently
133 formed invasive hyphae (not shown). However, *ece1Δ/Δ+ECE1_{Δ184-279}* was unable to induce
134 p-MKP1, c-Fos DNA binding, cytokines, or damage epithelia (Fig. 2f-i). In murine OPC,
135 unlike the *ece1Δ/Δ+ECE1* complemented strain, *ece1Δ/Δ+ECE1_{Δ184-279}*-infected mice
136 demonstrated absent (n = 4/10) or low (n = 6/10) fungal burdens, with no evidence of
137 inflammatory infiltrates or local epithelial damage (Fig. 2j-l, Extended Data Fig. 4a and 4b)

138 Likewise, *ece1* Δ/Δ +*ECEI*₁₈₄₋₂₇₉ did not induce full damage in the zebrafish swimbladder
139 model (Fig. 2m, Extended Data Fig. 4c). In contrast, injection of lytic doses of Ece1-III₆₂₋₉₃
140 into the swimbladder induced epithelial damage (Fig. 2n, o). Thus, Ece1-III₆₂₋₉₃ is both
141 necessary and sufficient for epithelial immune activation, damage and mucosal infection *in*
142 *vivo*. The amphipathic properties of Ece1-III₆₂₋₉₃
143 (SIIGIIMGILGNIPQVIQIIMSIVKAFKGNKR) coupled with the α -helical structure of the
144 N-terminal hydrophobic region (Extended Data Fig. 5a, b) indicated that this fungal peptide
145 may act similarly to cationic antimicrobial peptides and peptide toxins such as melittin²²
146 (honey bee), magainin²³ (African clawed frog) and alamethicin²⁴ (*Trichoderma viride*).
147 Cytolytic peptide toxins have not previously been found in human pathogenic fungi but
148 bacterial cytolytic toxins are known to induce lesions after binding to target cell
149 membranes^{25,26}. To investigate the importance of lipid composition for Ece1-III₆₂₋₉₃-
150 mediated cytolysis, we used Förster resonance energy transfer (FRET) and electrical
151 impedance spectroscopy to analyze the interactions of Ece1-III₆₂₋₉₃ with model membranes
152 comprised of lipid bilayers of dioleoylphosphatidylcholine (DOPC) with or without
153 cholesterol. While Ece1-III₆₂₋₉₃ was able to efficiently intercalate into and permeabilize
154 DOPC membranes, Ece1-III₆₂₋₉₃ permeabilization was enhanced in the presence of
155 cholesterol (Fig. 3a, Extended Data Fig. 5c). Ece1-III₆₂₋₉₃-induced lesions were
156 heterogeneous and transient (Extended Data Fig. 5d), indicating that the peptide may damage
157 target membranes through a ‘carpet-like’ mechanism²⁷. Patch-clamp analysis of epithelial
158 cells demonstrated that lesion formation by Ece1-III₆₂₋₉₃ is rapid and causes an inward current
159 (Fig. 3b), associated with calcium influx (Fig. 3c). Similar phenomena occur with bacterial
160 cytolytic toxins, which are known to trigger cell activation^{25,26,28}.

161 We postulated that the positively-charged C-terminal KR residues of Ece1-III₆₂₋₉₃ might
162 be critical for interacting with negatively-charged components of host membranes to promote
163 lesion formation. Substitution of the KR motif to AA (alanine-alanine; Ece1-III_{62-93AA}) did
164 not affect membrane intercalation (not shown) but significantly reduced the peptide’s ability
165 to permeabilize membranes, damage epithelial cells and induce calcium influx (Fig. 3c-e).
166 Thus, the positive C-terminus of Ece1-III₆₂₋₉₃ is critical for lesion formation and damage
167 induction in epithelial membranes. Notably, Ece1-III_{62-93AA} still induced p-MKP1, c-Fos and
168 the non-damage associated cytokine G-CSF (Fig. 3f, g) but not the damage-associated
169 cytokine IL-1 α (Fig. 3h), suggesting that Ece1-III_{62-93AA} can be recognized by epithelial
170 immunity without damaging cells. This finding is important as it means that epithelial cells
171 are not only responding to damage but have evolved to specifically recognise the peptide.

172

173 **Ece1-III_{62-92K} is a secreted cytolytic peptide toxin**

174 To demonstrate that Ece1-III is generated during epithelial infection, we performed LC-
175 MS/MS analysis on the secretome from wild-type *C. albicans* hyphae grown in the presence
176 and absence of epithelial cells (Supplementary information). Notably, Ece1-III was the only
177 peptide detected in the presence of epithelial cells, indicating that the fungus secretes this
178 toxin during mucosal infection. However, the predominant form of secreted Ece1-III
179 terminated in a K residue (SIIGIIMGILGNIPQVIQIIMSIVKAFKGNK; Ece1-III_{62-92K}) and
180 not KR (SIIGIIMGILGNIPQVIQIIMSIVKAFKGNKR; Ece1-III_{62-93KR}) (Extended Data
181 Table 3). In fungi, it is known that following Kex2p processing, many proteins are
182 subsequently cleaved by Kex1p²⁹ (also in the Golgi), removing the C-terminal R. LC-
183 MS/MS analysis on the hyphal secretome of a *kex1Δ/Δ* mutant demonstrated that the
184 predominant peptide secreted terminates in KR (not K) (Supplementary information).
185 Therefore, Ece1p is also subject to ordered Kex2p/Kex1p processing. Accordingly, we
186 confirmed that Ece1-III_{62-92K} functioned similarly to Ece1-III_{62-93KR} with respect to epithelial
187 cell activation. Specifically, Ece1-III_{62-92K} is also α -helical (not shown) and induces c-Fos, p-
188 MKP1, cytokines (IL-1 α , G-CSF), damage (LDH), membrane intercalation and
189 permeabilization, and calcium influx (Fig 4a-g). Thus, the dominant peptide secreted from *C.*
190 *albicans* hyphae during mucosal infection is Ece1-III_{62-92K}, which acts as a cytolytic peptide
191 toxin that activates epithelial cells.

192 Based on these data, we propose a model of *C. albicans* mucosal infection whereby
193 invasive hyphae secrete Ece1-III_{62-92K} into a membrane-bound ‘invasion pocket’^{30,31},
194 facilitating peptide accumulation (Extended Data Fig 6). During early stages of infection,
195 sub-lytic concentrations of Ece1-III_{62-92K} induce epithelial immunity by activating the ‘danger
196 response’ pathway (p-MKP1/c-Fos), alerting the host to the transition from colonizing yeast
197 to invasive, toxin-producing hyphae. As infection progresses, Ece1-III_{62-92K} levels
198 accumulate and elicit direct tissue damage. Mechanistically, we propose that the asymmetric
199 distribution of charge along the α -helix of Ece1-III_{62-92K} facilitates correct peptide orientation
200 relative to the host membrane, enabling intercalation, permeabilization and calcium influx.
201 In conclusion, our data identifies *C. albicans* Ece1-III_{62-92K} as the first cytolytic peptide toxin
202 in a human fungal pathogen and reveals the molecular mechanisms of epithelial damage and
203 host recognition of this clinically important fungus. We propose the name ‘Candidalysin’ for
204 this newly discovered fungal toxin.

205

206 **Supplementary Information** is available in the online version of the paper.

207

208 **Acknowledgements** We thank Sarah Gaffen, Bruce Klein, Christian Hertweck, Abigail
209 Tucker, Jeremy Green and Stephen Challacombe for comments on the manuscript. For
210 experimental assistance we thank Stuart Bevan and David Andersson (calcium assays),
211 Deepa Nayar (histology), Durdana Rahman and Mukesh Mistry (murine model), Mark Nilan
212 (zebrafish model), Sabrina Groth (FRET spectroscopy), Nadine Gebauer (Impedance
213 experiments), Daniela Schulz (*kex1Δ/Δ* strain) and our colleagues for supplying fungal
214 mutant strains. This work was supported by grants from the Medical Research Council
215 (MR/J008303/1, MR/M011372/1), Biotechnology & Biological Sciences Research Council
216 (BB/J015261/1), FP7-PEOPLE-2013-Initial Training Network (606786) to JRN; Wellcome
217 Trust Strategic Award for Medical Mycology and Fungal Immunology (097377/Z/11/Z) to
218 JRN and DW; Sir Henry Dale Fellowship jointly funded by the Wellcome Trust and the
219 Royal Society (102549/Z/13/Z) to DW; Deutsche Forschungsgemeinschaft CRC/TR124
220 FungiNet Project C1 and Z2, Deutsche Forschungsgemeinschaft SPP 1580 (Hu 528/17-1) and
221 CSCC, German Federal Ministry of Education and Health [BMBF] 01EO1002 to BH; Cluster
222 of Excellence ‘Inflammation at interfaces’ and Deutsche Forschungsgemeinschaft SPP1580
223 project GU 568/5-1 to TG; National Institutes of Health (R15AI094406) and the Burroughs
224 Wellcome Fund to RTW.

225

226 **Author Contributions** DLM, JPR, SXT, MR, CM, MB, SII, NK performed signaling,
227 transcription factor, calcium and cytokine assays, and murine work; DW, SH, SM, TMF,
228 BHe, LK AH, OB and OKu created fungal strains and performed fluorescent microscopy,
229 adhesion, invasion, gene expression and damage assays; RLG and RTW performed zebrafish
230 experiments; JW and TG performed biophysical analysis with artificial membranes; JR
231 performed whole patch clamp analysis; GV performed electron microscopy; ST performed
232 histological analysis; SM, TL, TK and OKn performed LC-MS analyses; JRN, BHu, DLM,
233 JPR and DW wrote the paper; JRN, BHu and EC supervised the project.

234

235 **Author Information** Reprints and permissions information is available at
236 www.nature.com/reprints. The authors declare no competing financial interests. Readers are
237 welcome to comment on the online version of the paper. Correspondence and requests for
238 materials should be addressed to BH (bernhard.hube@leibniz-hki.de).

239

240 **References**

- 241 1 Brown, G. D. *et al.* Hidden killers: human fungal infections. *Sci Transl Med* **4**, 165rv113
242 (2012).
- 243 2 Jacobsen, I. D. *et al.* *Candida albicans* dimorphism as a therapeutic target. *Expert Rev*
244 *Anti Infect Ther* **10**, 85-93 (2012).
- 245 3 Moyes, D. L. *et al.* A Biphasic Innate Immune MAPK Response Discriminates
246 between the Yeast and Hyphal Forms of *Candida albicans* in Epithelial Cells. *Cell*
247 *Host Microbe* **8**, 225-235 (2010).
- 248 4 Moyes, D. L. *et al.* *Candida albicans* yeast and hyphae are discriminated by MAPK
249 signaling in vaginal epithelial cells. *PLoS ONE* **6**, e26580 (2011).
- 250 5 Murciano, C. *et al.* *Candida albicans* cell wall glycosylation may be indirectly
251 required for activation of epithelial cell proinflammatory responses. *Infect.Immun* **79**,
252 4902-4911 (2011).
- 253 6 Moyes, D. L. *et al.* Activation of MAPK/c-Fos induced responses in oral epithelial
254 cells is specific to *Candida albicans* and *Candida dubliniensis* hyphae. *Med Microbiol*
255 *Immunol* **201**, 93-101 (2012).
- 256 7 Murciano, C. *et al.* Evaluation of the role of *Candida albicans* agglutinin-like
257 sequence (Als) proteins in human oral epithelial cell interactions. *PLoS ONE* **7**,
258 e33362 (2012).
- 259 8 Moyes, D. L. & Naglik, J. R. Mucosal Immunity and *Candida albicans* Infection.
260 *Clinical and Devel Immunol* **2011** (2011).
- 261 9 Naglik, J. R. & Moyes, D. Epithelial Cell Innate Response to *Candida albicans*. *Adv*
262 *Dent Res* **23**, 50-55 (2011).
- 263 10 Naglik, J. R., Moyes, D. L., Wachtler, B. & Hube, B. *Candida albicans* interactions
264 with epithelial cells and mucosal immunity. *Microbes Infect.* **13**, 963-976 (2011).
- 265 11 Hebecker, B., Naglik, J. R., Hube, B. & Jacobsen, I. D. Pathogenicity mechanisms
266 and host response during oral *Candida albicans* infections. *Expert Rev Anti Infect*
267 *Ther* **12**, 867-879 (2014).
- 268 12 Naglik, J. R. *Candida* Immunity. *New Journal of Science* **2014**, Article ID 390241,
269 390227 pages. doi:390210.391155/392014/390241 (2014).
- 270 13 Naglik, J. R., Richardson, J. P. & Moyes, D. L. *Candida albicans* Pathogenicity and
271 Epithelial Immunity. *PLoS Pathog* **10**, e1004257 (2014).

- 272 14 Moyes, D. L., Richardson, J. P. & Naglik, J. R. *Candida albicans*-epithelial
273 interactions and pathogenicity mechanisms: scratching the surface. *Virulence* **6**, 338-
274 346 (2015).
- 275 15 Birse, C. E., Irwin, M. Y., Fonzi, W. A. & Sypherd, P. S. Cloning and
276 characterization of *ECE1*, a gene expressed in association with cell elongation of the
277 dimorphic pathogen *Candida albicans*. *Infect Immun* **61**, 3648-3655 (1993).
- 278 16 Rohm, M. *et al.* A family of secreted pathogenesis-related proteins in *Candida*
279 *albicans*. *Mol Microbiol* **87**, 132-151 (2013).
- 280 17 Kamai, Y., Kubota, M., Hosokawa, T., Fukuoka, T. & Filler, S. G. New model of
281 oropharyngeal candidiasis in mice. *Antimicrob Agents and Chemother* **45**, 3195-3197
282 (2001).
- 283 18 Brothers, K. M. *et al.* NADPH Oxidase-Driven Phagocyte Recruitment Controls
284 *Candida albicans* Filamentous Growth and Prevents Mortality. *PLoS Pathog* **9**,
285 e1003634 (2013).
- 286 19 Gratacap, R. L., Rawls, J. F. & Wheeler, R. T. Mucosal candidiasis elicits NF-kappaB
287 activation, proinflammatory gene expression and localized neutrophilia in zebrafish.
288 *Dis Model Mech* **6**, 1260-1270 (2013).
- 289 20 Bader, O., Krauke, Y. & Hube, B. Processing of predicted substrates of fungal Kex2
290 proteinases from *Candida albicans*, *C. glabrata*, *Saccharomyces cerevisiae* and
291 *Pichia pastoris*. *BMC Microbiol* **8**, 116 (2008).
- 292 21 Newport, G. & Agabian, N. *KEX2* influences *Candida albicans* proteinase secretion
293 and hyphal formation. *J Biol Chem* **272**, 28954-28961 (1997).
- 294 22 Liu, P., Huang, X., Zhou, R. & Berne, B. J. Observation of a dewetting transition in
295 the collapse of the melittin tetramer. *Nature* **437**, 159-162 (2005).
- 296 23 Bechinger, B. & Salnikow, E. S. The membrane interactions of antimicrobial peptides
297 revealed by solid-state NMR spectroscopy. *Chem Phys Lipids* **165**, 282-301 (2012).
- 298 24 Pieta, P., Mirza, J. & Lipkowski, J. Direct visualization of the alamethicin pore
299 formed in a planar phospholipid matrix. *Proc Natl Acad Sci U S A* **109**, 21223-21227
300 (2012).
- 301 25 Bischofberger, M., Iacovache, I. & van der Goot, F. G. Pathogenic pore-forming
302 proteins: function and host response. *Cell Host Microbe* **12**, 266-275 (2012).
- 303 26 Los, F. C., Randis, T. M., Aroian, R. V. & Ratner, A. J. Role of pore-forming toxins
304 in bacterial infectious diseases. *Microbiol Mol Biol Rev* **77**, 173-207 (2013).

305 27 Oren, Z. & Shai, Y. Selective lysis of bacteria but not mammalian cells by
306 diastereomers of melittin: structure-function study. *Biochem* **36**, 1826-1835 (1997).

307 28 Walev, I. *et al.* Delivery of proteins into living cells by reversible membrane
308 permeabilization with streptolysin-O. *Proc Natl Acad Sci U S A* **98**, 3185-3190
309 (2001).

310 29 Schmitt, M. J. & Breinig, F. Yeast viral killer toxins: lethality and self-protection. *Nat*
311 *Rev Microbiol* **4**, 212-221 (2006).

312 30 Zakikhany, K. *et al.* In vivo transcript profiling of *Candida albicans* identifies a gene
313 essential for interepithelial dissemination. *Cell Microbiol* **9**, 2938-2954 (2007).

314 31 Wachtler, B. *et al.* *Candida albicans*-epithelial interactions: dissecting the roles of
315 active penetration, induced endocytosis and host factors on the infection process.
316 *PLoS ONE* **7**, e36952 (2012).

317

318 **Figure Legends**

319 **Figure 1| *ECE1* is required for epithelial activation and *C. albicans* infection.** TR146
320 cells were infected with the indicated *C. albicans* strains. **(a)** LDH release 24 h post-infection
321 (p.i.) (MOI = 0.1). **(b)** Induction of p-MKP-1 and c-Fos at 2 h p.i. (MOI = 10). **(c)** c-Fos
322 DNA binding at 3 h p.i. (MOI = 10). **(d)** G-CSF production at 24 h p.i. (MOI = 0.01). **(e-i)**
323 PAS-stained tongues from mice subjected to OPC 2 d p.i. **(e, g, h)** Whole-mount (x25) and **(f,**
324 **i)** high-power (x200) views of PAS-stained tongues of mice infected with *C. albicans* wild
325 type **(e, f)**, *ece1* Δ/Δ **(g)** and *ece1* Δ/Δ +*ECE1* **(h, i)**. Invading hyphae (black arrow) and
326 inflammatory cells (blue arrow) are indicated. **(j)** Quantification of neutrophils in zebrafish
327 swimbladder following infection with WT *C. albicans* (n (number of fish) = 47), *ece1* Δ/Δ (n
328 = 53) or PBS (n = 40). **(k)** Quantification of damaged cells in zebrafish swimbladder after
329 infection with *C. albicans* WT (n = 73), *ece1* Δ/Δ (n = 59) or vehicle (n = 63). Data are
330 representative **(b, e-i)** or the mean **(a, c-d, j-k)** of three biological replicates. Error bars \pm
331 SEM. Data were analyzed by one-way ANOVA **(a, d)**, paired T test **(c)** or Kruskal-Wallis **(j,**
332 **k)** and * = $P < 0.05$, ** = $P < 0.01$, *** = $P < 0.001$. For gel source data, see Supplementary
333 Figure 1.

334

335 **Figure 2| *Ece1-III*₆₂₋₉₃ is the active region of *Ece1p* and is required for TR146 cell**
336 **activation and mucosal *C. albicans* infection.** **(a)** Induction of p-MKP-1 and c-Fos 2 h post-
337 stimulation (p.s.) with *Ece1* peptides at 1.5 μ M. **(b)** LDH release 24 h p.s. with 70 μ M *Ece1*
338 peptides. **(c)** Induction of G-CSF 24 h p.s. of with *Ece1-III*₆₂₋₉₃. **(d)** c-Fos DNA binding
339 induction 3 h p.s. with sub-lytic concentrations of *Ece1-III*₆₂₋₉₃. **(e)** LDH release 24 h p.s. with
340 *Ece1-III*₆₂₋₉₃. **(f)** Induction of p-MKP-1 and c-Fos 2 h post-infection (p.i.) with the indicated
341 *C. albicans* strains (MOI = 10). **(g)** c-Fos DNA binding induction 3 h p.i. with indicated *C.*
342 *albicans* strains (MOI = 10). **(h)** G-CSF secretion 24 h p.i. with indicated *C. albicans* strains
343 (MOI = 0.01). **(i)** LDH release 24 h p.i. with indicated *C. albicans* strains (MOI = 0.01). **(j-l)**
344 PAS stained tongue sections from mice subjected to OPC, 2 d p.i. with **(j, k)** *C. albicans*
345 *ece1* Δ/Δ +*ECE1* (x25 and x200) or **(l)** *ece1* Δ/Δ +*ECE1* _{Δ 184-279}. Invading hyphae (black
346 arrows) and infiltrating inflammatory cells (blue arrow) are shown. **(m)** Damaged cells in a
347 zebrafish swimbladder 24 h p.i. with *C. albicans ece1* Δ/Δ +*ECE1* (n (number of fish) = 44),
348 *ece1* Δ/Δ +*ECE1* _{Δ 184-279} (n = 58) or vehicle (n = 58). **(n)** Damaged cells in zebrafish
349 swimbladders after stimulation with 9 ng (n = 51) or 1.25 ng (n = 56) *Ece1-III*₆₂₋₉₃, or vehicle
350 (40% DMSO, n = 54 and 5% DMSO, n = 55). **(o)** Co-localization of adherens junctions (α -

351 catenin-citrine) with Ece1-III₆₂₋₉₃-damaged cells (Sytox Orange-positive cells) in a zebrafish
352 swimbladder. Data are representative (**a, f, j-l, o**) or mean (**b-e, g-i, m-n**) of three biological
353 replicates (**a-m**) or ten fish (**o**). Error bars show \pm SEM. Data were analyzed by one-way
354 ANOVA (**b, c, e, h, i**) paired T test (**d, g**) or Kruskal-Wallis (**m,n**). * = $P < 0.05$, ** = $P <$
355 0.01 , *** = $P < 0.001$ (compared with vehicle control unless otherwise indicated). For gel
356 source data, see Supplementary Figure 1.

357

358 **Figure 3| Ece1-III₆₂₋₉₃ functions as a cytolytic peptide toxin.** (**a**) Kinetic changes in
359 conductance of tethered lipid membranes after exposure to different concentrations of Ece1-
360 III₆₂₋₉₃. (**b**) Evoked inward current at a membrane potential of -60 mV in TR146 cells post-
361 addition of Ece1-III₆₂₋₉₃ or ionomycin (positive control); individual (representative) and
362 cumulative changes (bar chart - number of cells analysed below each bar) shown. (**c**)
363 Intracellular calcium level kinetics in TR146 cells post-stimulation (p.s.) with Ece1-III₆₂₋₉₃
364 wild type (Ece1-III_{62-93KR}) or Ece1-III₆₂₋₉₃ AA C-terminal substitution (Ece1-III_{62-93AA}). (**d**)
365 Kinetic changes in conductance of tethered DOPC membranes after exposure to different
366 concentrations of Ece1-III₆₂₋₉₃. (**e**) LDH release from TR146 cells 24 h p.s. with Ece1-III₆₂₋₉₃
367 _{93KR} or Ece1-III_{62-93AA}. (**f**) Induction of p-MKP-1 and c-Fos 2 h in TR146 cells p.s. with Ece1-
368 III_{62-93KR} or Ece1-III_{62-93AA}. Secretion of (**g**) G-CSF and (**h**) IL-1 α from TR146 cells 24 h p.s.
369 with Ece1-III_{62-93KR} or Ece1-III_{62-93AA}. Data shown are representative (**a, d, f**) or mean (**b-c, e,**
370 **g-h**) of three biological replicates. Error bars show \pm SEM. Data were analyzed by one-way
371 ANOVA (**e, g** and **f**) and * = $P < 0.05$, ** = $P < 0.01$, *** = $P < 0.001$. For gel source data,
372 see Supplementary Figure 1.

373

374 **Figure 4| Ece1-III_{62-92K} functions as a cytolytic peptide toxin that activates and damages**
375 **epithelial cells.** (**a**) Induction of p-MKP-1 and c-Fos 2 h post-stimulation (p.s.), and (**b**)
376 secretion of G-CSF and IL-1- α 24 h p.s., and (**c**) LDH release 24 h p.s. of TR146 cells with
377 Ece1-III_{62-92K}. (**d**) Förster resonance energy transfer (FRET) showing intercalation of Ece1-
378 III_{62-92K} (10 μ M) into lipid liposomes. (**e**) Average peptide concentration-dependent changes
379 in conductance of tethered lipid membranes. (**f**) Ece1-III_{62-92K} (4 μ M) induced
380 permeabilization of planar lipid membranes showing heterogeneous and transient lesions
381 leading to membrane rupture. (**g**) Intracellular calcium level kinetics in TR146 cells p.s. with
382 Ece1-III_{62-92K}. Data shown are representative (**a, d, f**) or mean (**b-c, e, g**) of three biological
383 replicates. Error bars show \pm SEM. Data are analyzed by one-way ANOVA (**b, c**). * = $P <$

384 0.05, ** = $P < 0.01$, *** = $P < 0.001$ (compared with vehicle control). For gel source data,
385 see Supplementary Figure 1.

386

387 **Extended Data Figure legends**

388

389 **Extended Data Figure 1| *C. albicans* *ECE1* expression and phenotypic effects of *ECE1***
390 **gene deletion. (a)** Relative expression (vs $t = 0$) of *ECE1* in *C. albicans* wild type over time
391 after addition of yeast cells to TR146 epithelial cells as measured by RT-qPCR. **(b)** Imaging
392 confirmation of *ECE1* expression over time within *C. albicans* wild type. *C. albicans* cells
393 expressing GFP under the control of the *ECE1* 5' intragenic region, containing the *ECE1*
394 promoter, were grown on TR146 epithelial cells and stained with calcofluor white (CFW,
395 post-permeabilization) to show cell wall chitin and Alexa-Fluor-647-labelled concanavalin A
396 (ConA, pre-permeabilization) to show carbohydrates. A composite image showing CFW,
397 ConA, GFP and the brightfield (BF) image is shown. **(c)** Scanning electron micrographs (top
398 panels, 5 h) and light microscopy (bottom panels, 24 h) showing no gross abnormalities in
399 hypha formation between *C. albicans* wild type (BWP17+CIp30), *ECE1*-deletion (*ece1Δ/Δ*)
400 and *ECE1* re-integrand (*ece1Δ/Δ+ECE1*) strains after infection of TR146 epithelial cells. **(d)**
401 No difference in adhesion of *C. albicans* wild type, *ece1Δ/Δ* and *ece1Δ/Δ+ECE1* strains to
402 TR146 epithelial cells after 60 min. **(e)** No difference in invasion of *C. albicans* wild type,
403 *ece1Δ/Δ* and *ece1Δ/Δ+ECE1* strains into TR146 epithelial cells after 3 h. **(f)** Fluorescence
404 staining of *C. albicans* wild type and *ece1Δ/Δ* hyphae invading through TR146 epithelial
405 cells. Fungal cells are stained with calcofluor white (CFW, post-permeabilization) and Alexa-
406 Fluor-647-labelled concanavalin A (ConA, pre-permeabilization) to show cell wall chitin and
407 carbohydrates, respectively, and to distinguish between invading hyphae (only stained after
408 permeabilization) and non-invading hyphae (stained both pre- and post-permeabilization).
409 Levels of chitin and β -glucan are comparable in both strains. White arrows indicate invasion
410 into epithelial cells. Data shown are representative **(b, c, f)** or the mean **(a, d, e)** of three
411 biological replicates. Error bars show \pm SEM.

412

413 **Extended Data Figure 2| *C. albicans* Ece1p is critical for mucosal virulence *in vivo*. (a)**
414 Fungal burdens recovered from the tongues of mice infected with *C. albicans* wild type
415 (BWP17+CIp30) ($n = 13$), *ECE1*-deletion (*ece1Δ/Δ*) (n (number of mice) = 20) and *ECE1* re-
416 integrand (*ece1Δ/Δ+ECE1*) ($n = 24$) strains after 2 day oropharyngeal infection. **(b)** Average

417 percentage of the entire tongue epithelium area infected in different groups of mice infected
418 with the different *C. albicans* strains. **(c)** Confocal imaging of 4 day post-fertilization (dpf)
419 *mpo-gfp* transgenic zebrafish swimbladders infected with *C. albicans* wild type
420 (BWP17+Cip30+dTomato), *ECE1*-deletion (*ece1Δ/Δ+dTomato*) and *ECE1* re-integrant
421 (*ece1Δ/Δ+ECE1+dTomato*) strains for 24 h. *C. albicans* cells appear red whilst neutrophils
422 appear green. Red dots outline the swimbladder. Images are composites of maximum
423 projections in the red and green channels (25 slices each, approximately 100 μm depth) with
424 (left) or without (right) a single slice in the DIC channel overlay. Scale bars represent 100
425 μm. **(d)** Confocal imaging of 4 dpf zebrafish swimbladders infected with *C. albicans* wild
426 type (BWP17+Cip30+dTomato), *ECE1*-deletion (*ece1Δ/Δ+dTomato*) and *ECE1* re-integrant
427 (*ece1Δ/Δ+ECE1+dTomato*) strains for 24 h stained with the fluorescent exclusion dye Sytox
428 Green. *C. albicans* cells appear red and damaged epithelial cells appear green. White dots
429 outline the pronephros and red dots outline the swimbladder. Images are composites of
430 maximum projections in the red and green channels (25 slices each, approximately 100 μm
431 depth) with (left) or without (right) a single slice in the DIC channel overlay. High
432 magnification images of the white boxes are shown. Scale bars (bottom right) represent 100
433 μm (low magnification) and 30 μm (high magnification). Data shown are the mean **(a, b)** or
434 representative **(c, d)** of at least three biological replicates. Error bars show ± SEM. Data were
435 analyzed by Mann-Whitney test. *** = $P < 0.001$.

436

437 **Extended Data Figure 3| Ece1-III₆₂₋₉₃ is the active region of Ece1p.** **(a)** Amino acid
438 sequence of Ece1p and a schematic of the protein, indicating the signal peptide (SP), lysine-
439 arginine motifs (KR) at the C-terminus of each peptide, and the processed peptides (Ece1-I-
440 VIII) produced by Kex2p cleavage. **(b)** Amino acid sequences of the processed peptides
441 (Ece1-I-VIII) produced by Kex2p cleavage. Induction of **(c)** GM-CSF, **(d)** IL-1α and **(e)** IL-6
442 secreted after stimulation of TR146 epithelial cells for 24 h with varying concentrations of
443 Ece1-III₆₂₋₉₃ (70 μM - 1.5 μM). **(f)** Phosphorylation of MKP-1 and c-Fos production after 2 h
444 treatment of TR146 epithelial cells with 15 μM of Ece1-III₆₂₋₈₅ (hydrophobic region), Ece1-
445 III₈₆₋₉₃ (hydrophilic region), Ece1-III₆₂₋₈₅ and Ece1-III₈₆₋₉₃ together, or Ece1-III₆₂₋₉₃ alone. **(g)**
446 Induction of G-CSF secretion after 24 h treatment of TR146 epithelial cells with 15 μM of
447 Ece1-III₆₂₋₈₅, Ece1-III₈₆₋₉₃, Ece1-III₆₂₋₈₅ and Ece1-III₈₆₋₉₃ together, or Ece1-III₆₂₋₉₃ alone. **(h)**
448 Fold change induction of LDH release after 24 h treatment of TR146 epithelial cells with 70
449 μM of Ece1-III₆₂₋₈₅, Ece1-III₈₆₋₉₃, Ece1-III₆₂₋₈₅ and Ece1-III₈₆₋₉₃ together, or Ece1-III₆₂₋₉₃
450 alone. Data shown are representative **(f)** or the mean **(c-e, g-h)** of three biological replicates.

451 Error bars show \pm SEM. Data were analyzed by one-way ANOVA. * = $P < 0.05$, ** = $P <$
452 0.01, *** = $P < 0.001$ (compared with vehicle control). For gel source data, see
453 Supplementary Figure 1.

454

455 **Extended Data Figure 4| Ece1-III₆₂₋₉₃ is required for *C. albicans* mucosal infection. (a)**

456 Fungal burdens recovered from the tongues of mice infected with *C. albicans* wild type

457 (BWP17+CIp30) (n = 13), *ECE1*-deletion (*ece1 Δ / Δ*) (n = 20), *ECE1* re-integrant

458 (*ece1 Δ / Δ +ECE1*) (n = 24) and Ece1-III₆₂₋₉₃ deletion (*ece1 Δ / Δ +ECE1 $_{\Delta 184-279}$*) (n = 10) strains

459 after 2 day oropharyngeal infection. (b) Average percentage of the entire tongue epithelium

460 area infected in different groups of mice infected with the different *C. albicans* strains. (c)

461 Confocal imaging of 4 dpf zebrafish swimbladders infected with *C. albicans* Ece1-III₆₂₋₉₃

462 deletion (*ece1 Δ / Δ +ECE1 $_{\Delta 184-279}$ +dTomato*) and *ECE1* re-integrant

463 (*ece1 Δ / Δ +ECE1+dTomato*) strains for 24 h stained with the fluorescent exclusion dye Sytox

464 Green. *C. albicans* cells appear red and damaged cells appear green. White dots outline the

465 pronephros and red dots outline the swimbladder. Images are composites of maximum

466 projections in the red and green channels (25 slices each, approximately 100 μ m depth) with

467 (left) or without (right) a single slice in the DIC channel overlay. Scale bars (bottom right)

468 represent 100 μ m. Data shown are the mean (a) or representative (b, c) of at least three

469 biological replicates. Error bars show \pm SEM. Data were analyzed by Mann-Whitney test. **

470 = $P < 0.01$, *** = $P < 0.001$.

471

472 **Extended Data Figure 5| Ece1-III₆₂₋₉₃ is a cytolytic α -helical peptide. (a)** Circular

473 dichroism spectra showing the α -helical conformation of Ece1-III₆₂₋₉₃ in buffer (100 mM

474 KCl, 5 mM HEPES, pH 7). Increasing the temperature from 25°C to 40°C did not affect the

475 stability of the α -helical structure. (b) Diagram to illustrate the amphipathic nature of Ece1-

476 III₆₂₋₉₃ (residues 62-78, left panel; residues 79-93, right panel). Residues with hydrophobic or

477 polar/charged side chains are displayed with a blue and white background, respectively.

478 Modified from output generated in PEPWHEEL ([http://emboss.bioinformatics.nl/cgi-](http://emboss.bioinformatics.nl/cgi-bin/emboss/pepwheel)

479 [bin/emboss/pepwheel](http://emboss.bioinformatics.nl/cgi-bin/emboss/pepwheel)). (c) Förster resonance energy transfer (FRET) experiments show the

480 intercalation of Ece1-III₆₂₋₉₃ into lipid liposomes (10 μ M) composed of DOPC in the absence

481 or presence of cholesterol. Peptide titration of Ece1-III₆₂₋₉₃ to liposomes showed slightly

482 enhanced intercalation for pure DOPC. (d) Ece1-III₆₂₋₉₃ induced the permeabilization of

483 planar lipid membranes composed of DOPC. The graph shows heterogeneous and transient

484 lesions leading finally to a rupture of the membrane. Ece1-III₆₂₋₉₃ concentration was 0.125
485 μ M. Data shown are representative of at least three biological replicates.

486

487 **Extended Data Figure 6 | Schematic of the role of Ece1-III in *C. albicans* infection of**
488 **epithelial cells.** During early stage infection of the mucosal surface by *C. albicans*, Ece1-III
489 (red α -helix) is secreted into the invasion pocket created by the invading hypha (**a**). Sub-lytic
490 concentrations of Ece1-III trigger epithelial signal transduction through MAPK, p38/MKP-1
491 and c-Fos (**b**) resulting in the production of immune regulatory cytokines (**c**). As the severity
492 of the infection increases, Ece1-III accumulates (**d**) and once lytic concentrations are reached,
493 causes membrane damage and the release of lactate dehydrogenase from the host epithelium
494 (**e**), concomitant with calcium influx (**f**). Epithelial signal transduction is maintained (**g**) and
495 additionally induces the release of damage associated cytokines, such as IL-1 α (**h**). Ece1-III
496 may also have activity on the epithelial surface outside of the invasion pocket and on
497 neighbouring cells not in contact with hyphae if Ece1-III is produced in sufficient
498 concentrations.

499

500

501 **METHODS**

502

503 **Cell lines, reagents and *Candida* strains**

504 Experiments were carried out using the TR146 buccal epithelial squamous cell carcinoma
505 line³² obtained from the European Collection of Authenticated Cell Cultures (ECACC) and
506 grown in Dulbecco's Modified Eagle's Medium (DMEM, Sigma-Aldrich) supplemented with
507 10% fetal bovine serum (FBS) and 1% penicillin-streptomycin. Cells were routinely tested
508 for mycoplasma contamination using mycoplasma-specific primers and were found to be
509 negative. Prior to stimulation, confluent TR146 cells were serum-starved overnight, and all
510 experiments were carried out in serum-free DMEM. *C. albicans* wild type strains included
511 the autotrophic strain BWP17+CIp30³³ and the parental strain SC5314³⁴. Other *C. albicans*
512 strains used and their sources are listed in Extended Data Tables 1 and 2. *C. albicans* cultures
513 were grown in YPD medium (1% yeast extract, 2% peptone, 2% dextrose) at 30°C overnight.
514 Cultures were washed in sterile PBS and adjusted to the required cell density. Antibodies to
515 phospho-MKP1 and c-Fos were from Cell Signalling Technologies (New England Biolabs
516 UK), mouse anti-human α -actin was from Millipore (UK), and goat anti-mouse and anti-
517 rabbit horseradish peroxidase (HRP)-conjugated antibodies were from Jackson
518 Immunologicals Ltd (Strattech Scientific, UK). Ece1p peptides were synthesized
519 commercially (Proteogenix (France) or Peptide Synthetics (UK)).

520

521 **Generation of *C. albicans* *ECE1* mutant strains**

522 *ECE1* deletion was performed as previously described³⁵. Deletion cassettes were generated
523 by PCR³⁶. Primers ECE1-FG and ECE1-RG were used to amplify pFA-HIS1 and pFA-ARG4
524 -based markers. *C. albicans* BWP17³⁷, was sequentially transformed³⁸ with the *ECE1*-HIS1
525 and *ECE1*-ARG4 deletion cassettes and then transformed with CIp10³⁹, yielding the *ece1* Δ/Δ
526 deletion strain. For complementation, the *ECE1* gene plus upstream and downstream
527 intergenic regions were amplified with primers ECE1-RecF3k and ECE1-RecR and cloned
528 into plasmid CIp10 at *Mlu*I and *Sal*I sites. This plasmid was transformed into the uridine
529 auxotrophic *ece1* Δ/Δ strain, yielding the *ece1* Δ/Δ +*ECE1* complemented strain. For
530 generation of the *ece1* Δ/Δ +*ECE1* $_{\Delta 184-279}$ strain, the CIp10-*ECE1* was amplified with primers
531 Pep3-F1 and Pep3-R1, digested with *Cla*I and re-ligated, yielding the CIp10+*ECE1* $_{\Delta 184-279}$
532 plasmid. This plasmid was transformed into the uridine auxotrophic *ece1* Δ/Δ strain, yielding
533 the *ece1* Δ/Δ +*ECE1* $_{\Delta 184-279}$ strain. All integrations were confirmed by PCR/sequencing and at
534 least two independent isogenic transformants were created to confirm results. *KEX1* deletion

535 was performed exactly as the *ECE1* deletion but using primers KEX1-FG and KEX1-RG for
536 creating the deletion cassette. Fluorescent strains of *ece1* Δ/Δ and BWP17 were constructed as
537 previously described⁴⁰. Briefly, the *ece1* Δ/Δ and BWP17 strains were transformed with the
538 pENO1-dTom-NATr plasmid. Primers used to clone and construct the *ECE1* genes and
539 intragenic regions are listed in Extended Data Table 4. Strains are listed in Extended Data
540 Table 2.

541

542 **Construction of *C. albicans* *ECE1* promoter-GFP strain**

543 *ECE1* promoter (primers 5'*ECE1*prom-NarI / 3'*ECE1*prom-XhoI) and terminator
544 (5'*ECE1*term-SacII / 5'*ECE1*term-SacI) were amplified and cloned into pADH1-GFP.
545 Resulting pSK-p*ECE1*-GFP was verified by sequencing. *C. albicans* SC5314 was
546 transformed with the p*ECE1*-GFP transformation cassette³⁸. Resistance to nourseothricin was
547 used as selective marker and correct integration of GFP into the *ECE1* locus was verified by
548 PCR. Primers for cloning and validation are listed in Extended Data Table 4. Strains are
549 listed in Extended Data Table 2.

550

551 **RNA isolation and real-time PCR analysis**

552 *C. albicans* cells grown on TR146 epithelial cells were collected into RNA pure (PeqLab),
553 centrifuged and the pellet resuspended in 400 μ l AE buffer (50 mM Na-acetate pH 5.3, 10
554 mM EDTA, 1% SDS). Samples were vortexed (30 s), and an equal volume of
555 phenol/chloroform/isoamyl alcohol (25:24:1) was added and incubated for 5 min (65°C)
556 before subjected to 2x freeze-thawing. Lysates were clarified by centrifugation and the RNA
557 precipitated with isopropyl alcohol/0.3 M sodium acetate by incubating for 1 h at -20°C.
558 Precipitated pellets were washed (2x 1 ml 70% ice-cold ethanol), resuspended in DEPC-
559 treated water and stored at -80°C. RNA integrity and concentration was confirmed using a
560 Bioanalyzer (Agilent). RNA (500 ng) was treated with DNase (Epicenter) and cDNA
561 synthesized using Reverse Transcriptase Superscript III (Invitrogen). cDNA samples were
562 used for qPCR with EVAgreen mix (Bio&Sell). Primers (ACT1-F and ACT1-R for actin,
563 ECE1-F and ECE1-R for *ECE1* - Extended Data Table 4) were used at a final concentration
564 of 500 nM. qPCR amplifications were performed using a Biorad CFX96 thermocycler. Data
565 was evaluated using Bio-Rad CFX Manager 3.1 (Bio-Rad) with *ACT1* as the reference gene
566 and t_0 as the control sample.

567

568 **Western blotting**

569 TR146 cells were lysed using a modified RIPA lysis buffer (50 mM Tris-HCl pH 7.4, 150
570 mM NaCl, 1 mM EDTA, 1% Triton X-100, 1% sodium deoxycholate, 0.1% SDS) containing
571 protease (Sigma-Aldrich) and phosphatase (Perbio Science) inhibitors⁴¹, left on ice (30 min)
572 and then clarified (10 min) in a refrigerated microfuge. Lysate total protein content was
573 determined using the BCA protein quantitation kit (Perbio Science). 20 µg of total protein
574 was separated on 12% SDS-PAGE gels before transfer to nitrocellulose membranes (GE
575 Healthcare). After probing with primary (1:1000) and secondary (1:10,000) antibodies,
576 membranes were developed using Immobilon chemiluminescent substrate (Millipore) and
577 exposed to X-Ray film (Fuji film). Human α -actin was used as a loading control.

578

579 **Transcription factor DNA binding assay**

580 DNA binding activity of transcription factors was assessed using the TransAM transcription
581 factor ELISA system (Active Motif) as previously described^{41,42}. Serum-starved TR146
582 epithelial cells were treated for 3 h before being differentially lysed to recover nuclear
583 proteins using a nuclear protein extraction kit (Active Motif) according to the manufacturer's
584 protocol. Protein concentration was determined (BCA protein quantitation kit (Perbio
585 Science)) and 5 µg of nuclear extract was assayed in the TransAM system according to the
586 manufacturer's protocol. Data was expressed as fold-change in A_{450nm} relative to resting cells.

587

588 **Cytokine determination**

589 Cytokine levels in cell culture supernatants were determined using the Performance magnetic
590 Fluorokine MAP cytokine multiplex kit (Bio-technique) and a Bioplex 200 machine. The data
591 were analyzed using Bioplex Manager 6.1 software to determine analyte concentrations.

592

593 **Cell damage assay**

594 Following incubation, culture supernatant was collected and assayed for lactate
595 dehydrogenase (LDH) activity using the Cyttox 96 Non-Radioactive Cytotoxicity Assay kit
596 (Promega) according to the manufacturer's instructions. Recombinant porcine LDH (Sigma-
597 Aldrich) was used to generate a standard curve.

598

599 **Epithelial adhesion assay**

600 Quantification of *C. albicans* adherence to TR146 epithelial cells was performed as described
601 previously⁴³. Briefly, TR146 cells were grown to confluence on glass coverslips for 48 h in
602 tissue culture plates in DMEM medium. *C. albicans* yeast cells (2×10^5) were added into 1

603 ml serum-free DMEM, incubated for 60 min (37°C/5% CO₂) and non-adherent *C. albicans*
604 cells removed by aspiration. Following washing (3x 1 ml PBS), cells were fixed with 4%
605 paraformaldehyde (Roth) and adherent *C. albicans* cells stained with Calcofluor White and
606 quantified using fluorescence microscopy. The number of adherent cells was determined by
607 counting 100 high power fields of 200 µm × 200 µm size. Exact total cell numbers were
608 calculated based on the quantified areas and the total size of the cover slip.

609

610 **Epithelial invasion assay**

611 *C. albicans* invasion of epithelial cells was determined as described previously⁴³. Briefly,
612 TR146 epithelial cells were grown to confluence on glass coverslips for 48 h and then
613 infected with *C. albicans* yeast cells (1×10⁵), for 3 h in a humidified incubator (37°C/5%
614 CO₂). Following washing (3x PBS), the cells were fixed with 4% paraformaldehyde. All
615 surface adherent fungal cells were stained for 1 h with a rabbit anti-*Candida* antibody and
616 subsequently with a goat anti-rabbit-Alexa Fluor 488 antibody. After rinsing with PBS,
617 epithelial cells were permeabilized (0.1% Triton X-100 in PBS for 15 min) and fungal cells
618 (invading and non-invading) were stained with Calcofluor White. Following rinsing with
619 water, coverslips were visualized using fluorescence microscopy. The percentage of invading
620 *C. albicans* cells was determined by dividing the number of (partially) internalized cells by
621 the total number of adherent cells. At least 100 fungal cells were counted on each coverslip.

622

623 **Imaging of *C. albicans* growth and invasion of epithelial cells**

624 TR146 cells (10⁵/ml) seeded on glass coverslips in DMEM/10% FBS were infected with *C.*
625 *albicans* (2.5 × 10⁴ cfu/ml) in DMEM and incubated for 6 h (37°C/5% CO₂). Cells were
626 washed with PBS, fixed overnight (4°C in 4% paraformaldehyde) and stained with
627 Concanavalin A-Alexa Fluor 647 in PBS (10 µg/ml) for 45 min at room temperature in the
628 dark with gentle shaking (70 rpm) to stain the fungal cell wall. Epithelial cells were
629 permeabilised with 0.1% Triton X-100 for 15 min at 37°C in the dark, then washed and
630 stained with 10 µg/ml Calcofluor White (0.1 M Tris-HCl pH 9.5) for 20 min at room
631 temperature in the dark with gentle shaking. Cells were rinsed in water and mounted on slides
632 with 6 µl of ProLong Gold anti-fade reagent, before air drying for 2 h in the dark.
633 Fluorescence microscopy was performed on a Zeiss Axio Observer Z1 microscope, and 5
634 phase images were taken per picture.

635

636 **Scanning Electron Microscopy**

637 For scanning electron microscopy (SEM) analysis, TR146 cells were grown to confluence on
638 Transwell inserts (Greiner) and serum starved overnight in serum-free DMEM. After 5 h of
639 *C. albicans* incubation on epithelial cells at an MOI of 0.01, cell media was removed and
640 samples were fixed overnight at 4°C with 2.5% (v/v) glutaraldehyde in 0.05 M HEPES buffer
641 (pH 7.2) and post-fixed in 1% (w/v) osmium tetroxide for 1 h at room temperature. After
642 washing, samples were dehydrated through a graded ethanol series before being critical point
643 dried (Polaron E3000, Quorum Technologies Ltd). Dried samples were mounted using
644 carbon double side sticky discs (TAAB) on aluminium pins (TAAB) and gold coated in an
645 Emitech K550X sputter coater (Quorum Technologies Ltd). Samples were examined and
646 images recorded using a FEI Quanta 200 field emission scanning electron microscope
647 operated at 3.5 kV in high vacuum mode.

648

649 **Zebrafish swimbladder mucosal infection model**

650 Zebrafish infections were performed in accordance with NIH guidelines under Institutional
651 Animal Care and Use Committee (IACUC) protocol A2009-11-01 at the University of
652 Maine. To determine sample size, a power calculation was done for all experiments based on
653 2-tails T-test in order to detect a minimum effect size of 0.8, with an alpha error probability
654 of 0.05 and a power (1 – beta error probability) of 0.95. This gave a minimum number of 42
655 fish for each group. The fish selected for the experiments were randomly assigned to the
656 different groups by picking them from a pool without bias and the groups were injected in
657 different orders. No blinding was used to read the results. Ten to twenty zebrafish per group
658 per experiment were maintained at 33°C in E3 + PTU and used as previously described⁴⁰.
659 Briefly, 4 day post-fertilization (dpf) larvae were treated with 20 µg/ml dexamethasone
660 dissolved in 0.1% DMSO 1 h prior to infection and thereafter. For tissue damage and
661 neutrophil recruitment, individual AB or *mpo:GFP* fish (respectively) were injected into the
662 swimbladder with 4 nl of PBS with/without 25-40 *C. albicans* yeast cells of *ece1Δ/Δ-*
663 *dTomato*, *ece1Δ/Δ+ECE1+dTomato*, *ece1Δ/Δ+ECE1_{Δ184-279}+dTomato* or BWP17-*dTomato*.
664 For tissue damage, 1 nl of Sytox green (0.05 mM in 1% DMSO) was injected at 20 h post-
665 infection into the swimbladder and fish were imaged by confocal microscopy at 24 h post-
666 infection. For neutrophil recruitment, fish were imaged at 24 h post-injection. For synthetic
667 peptide damage, AB or α -catenin:citrine⁴⁴ fish were injected with 2 nl of peptide (9 ng or
668 1.25 ng per fish) or vehicle (40% DMSO or 5% DMSO) + SytoxGreen (0.05 mM in 1%
669 DMSO) or SytoxOrange (0.5 mM in 10% DMSO) and the fish imaged by confocal

670 microscopy 4 h later. Numbers of neutrophils and damaged cells observed were counted and
671 tabulated for each fish.

672

673 **Zebrafish swimbladder fluorescence microscopy**

674 Live zebrafish imaging was carried out as previously described⁴⁰. Briefly, fish were
675 anesthetized in Tris-buffered Tricaine (200 µg/ml, Western Chemicals) and further
676 immobilized in a solution of 0.4% low-melting-point agarose (LMA, Lonza) in E3 + Tricaine
677 in a 96-well plate glass-bottom imaging dish (Greiner Bio-On). Confocal imaging was carried
678 out using an Olympus IX-81 inverted microscope with an FV-1000 laser scanning confocal
679 system (Olympus). Images were collected and processed using Fluoview (Olympus) and
680 Photoshop (Adobe Systems Inc.). Panels are either a single slice for the differential
681 interference contrast channel (DIC) with maximum projection overlays of fluorescence image
682 channels (red-green), or maximum projection overlays of fluorescence channels. The number
683 of slices for each maximum projection is specified in the legend of individual figures.

684

685 **Murine oropharyngeal candidiasis model**

686 Murine infections were performed under UK Home Office Project Licence PPL 70/7598 in
687 dedicated animal facilities at King's College London. No statistical method was used to pre-
688 determine sample size. No method of randomization was used to allocate animals to
689 experimental groups. Mice in the same cage were part of the same treatment. The
690 investigators were not blinded during outcome assessment. A previously described murine
691 model of oropharyngeal candidiasis using female Balb/c mice⁴⁵ was modified for
692 investigating early infection events. Briefly, mice were treated sub-cutaneously with 3
693 mg/mouse (in 200 µl PBS with 0.5% Tween 80) of cortisone acetate on days -1 and 1 post-
694 infection. On day 0, mice were sedated for ~75 min with an intra-peritoneal injection of 110
695 mg/kg ketamine and 8 mg/kg xylazine, and a swab soaked in a 10⁷ cfu/ml *C. albicans* yeast
696 culture in sterile saline was placed sub-lingually for 75 min. After 2 days, mice were
697 sacrificed, the tongue excised and divided longitudinally in half. One half was weighed,
698 homogenized and cultured to derive quantitative *Candida* counts. The other half was
699 processed for histopathology and immunohistochemistry.

700

701 **Immunohistochemistry of murine tissue**

702 *C. albicans* infected murine tongues were fixed in 10% (v/v) formal-saline before being
703 embedded and processed in paraffin wax using standard protocols. For each tongue, 5 μ m
704 sections were prepared using a Leica RM2055 microtome and silane coated slides. Sections
705 were dewaxed using xylene, before *C. albicans* and infiltrating inflammatory cells were
706 visualized by staining using Periodic Acid-Schiff (PAS) stain and counterstaining with
707 haematoxylin. Sections were then examined by light microscopy. Histological quantification
708 of infection was undertaken by measuring the area of infected epithelium and expressed as a
709 percentage relative to the entire epithelial area.

710

711 **Whole cell patch clamp**

712 TR146 epithelial cells were grown in 35 mm petri dishes (Nunc) for 48 h before recordings at
713 low cell density (10-30% confluence). Cells were superfused with a modified Krebs solution
714 (120 mM NaCl, 3 mM KCl, 2.5 mM CaCl₂, 1.2 mM MgCl₂, 22.6 mM NaHCO₂, 11.1 mM
715 glucose, 5 mM HEPES pH 7.4). Isolated cells were recorded at room temperature (21-23°C)
716 in whole cell mode using microelectrodes (5-7 M Ω) containing 90 mM potassium acetate, 20
717 mM KCl, 40 mM HEPES, 3 mM EGTA, 3 mM MgCl₂, 1 mM CaCl₂ (free Ca²⁺ 40 nM), pH
718 7.4. Cells were voltage clamped at -60 mV using an Axopatch 200A amplifier (Axon
719 Instruments) and current/voltage curves were generated by 1 s steps between -100 to + 50
720 mV. Treatments were applied to the superfusate to produce the final required concentration,
721 with vehicle controls similarly applied. Data was recorded using Clampex software (PCLamp
722 6, Axon Instrument) and analyzed with Clampfit 10.

723

724 **Calcium flux**

725 TR146 cells were grown in a 96-well plate overnight until confluent. The medium was
726 removed and 50 μ l of a Fura-2 solution (5 μ l Fura-2 (Life Technologies)(2.5 mM in 50%
727 Pluronic F-127 (Life technologies):50% DMSO), 5 μ l probenecid (Sigma) in 5 ml saline
728 solution (NaCl (140 mM), KCl (5 mM), MgCl₂ (1 mM), CaCl₂ (2 mM), Glucose (10 mM)
729 and HEPES (10 mM), adjusted to pH 7.4)) was added and the plate incubated for 1 h at
730 37°C/5% CO₂. The Fura-2 solution was replaced with 50 μ l saline solution and baseline
731 fluorescence readings (excitation 340 nm/emission 520nm) taken for 10 min using a
732 FlexStation 3 (Molecular Devices). Ece1 peptides were added at different concentrations and
733 readings immediately taken for up to 3 h. The data was analyzed using Softmax Pro software
734 to determine calcium present in the cell cytosol and expressed as the ratio between excitation
735 and emission spectra.

736

737 **Impedance spectroscopy of tethered bilayer lipid membranes (tBLMs)**

738 tBLMs with 10% tethering lipids and 90% spacer lipids (T10 slides) were formed using the
739 solvent exchange technique^{46,47} according to the manufacturer's instructions (SDx Tethered
740 Membranes Pty Ltd, Sydney, Australia). Briefly, 8 μ l of 3 mM lipid solutions in ethanol were
741 added, incubated for 2 min and then 93.4 μ l buffer (100 mM KCl, 5 mM HEPES, pH 7.0)
742 was added. After rinsing 3x with 100 μ l buffer the conductance and capacitance of the
743 membranes were measured for 20 min before injection of Ece1 peptides at different
744 concentrations. All experiments were performed at room temperature. Signals were measured
745 using the tethaPod (SDx Tethered Membranes Pty Ltd, Sydney, Australia).

746

747 **FRET intercalation experiments**

748 Intercalation of Ece1 peptides into phospholipid liposomes was determined by FRET
749 spectroscopy applied as a probe-dilution assay⁴⁸. Phospholipids mixed with each 1%
750 (mol/mol) of the donor dye NBD-phosphatidylethanolamine (NBD-PE) and of the acceptor
751 dye rhodamine-PE, were dissolved in chloroform, dried, solubilized in 1 ml buffer (100 mM
752 KCl, 5 mM HEPES, pH 7.0) by vortexing, sonicated with a titan tip (30 W, Branson sonifier,
753 cell disruptor B15), and subjected to three cycles of heating to 60°C and cooling down to
754 4°C, each for 30 min. Lipid samples were stored at 4°C for at least 12 h before use. Ece1
755 peptide was added to liposomes and intercalation was monitored as the increase of the
756 quotient between the donor fluorescence intensity I_D at 531 nm and the acceptor intensity I_A
757 at 593 nm (FRET signal) independent of time.

758

759 **Circular Dichroism spectroscopy**

760 CD measurements were performed using a Jasco J-720 spectropolarimeter (Japan
761 Spectroscopic Co., Japan), calibrated as described previously⁴⁹. CD spectra represent the
762 average of four scans obtained by collecting data at 1 nm intervals with a bandwidth of 2 nm.
763 The measurements were performed in 100 mM KCl, 5 mM HEPES, pH 7.0 at 25°C and 40°C
764 in a 1.0 mm quartz cuvette. The Ece1-III concentration was 15 μ M.

765

766 **Planar lipid bilayers**

767 Planar lipid bilayers were prepared using the Montal-Mueller technique⁵⁰ as described
768 previously⁵¹. All measurements were performed in 5 mM HEPES, 100 mM KCl, pH 7.0
769 (specific electrical conductivity 17.2 mS/cm) at 37°C.

770

771 **Hyphal secretome preparation for LC-MS/MS analysis**

772 *Candida* strains were cultured for 18 h in hyphae inducing conditions (YNB medium
773 containing 2% sucrose, 75 mM MOPSO buffer pH 7.2, 5 mM N-acetyl-D-glucosamine,
774 37°C). Hyphal supernatants were collected by filtering through a 0.2 µm PES filter, and
775 peptides were enriched by Solid Phase Extraction (SPE) using first C4 and subsequently C18
776 columns on the C4 flowthrough. After drying in a vacuum centrifuge, samples were
777 resolubilised in loading solution (0.2% formic acid in 71:27:2 ACN/H₂O/DMSO (v/v/v)) and
778 filtered through a 10 kDa MWCO filter. The filtrate was transferred into HPLC vials and
779 injected into the LC-MS/MS system. LC-MS/MS analysis was carried out on an Ultimate
780 3000 nano RSLC system coupled to a QExactive Plus mass spectrometer (ThermoFisher
781 Scientific). Peptide separation was performed based on a direct injection setup without
782 peptide trapping using an Accucore C4 column as stationary phase and a column oven
783 temperature of 50°C. The binary mobile phase consisting of A) 0.2% (v/v) formic acid in
784 95:5 H₂O/DMSO (v/v) and B) 0.2% (v/v) formic acid in 85:10:5 ACN/H₂O/DMSO (v/v/v)
785 was applied for a 60 min gradient elution: 0-1.5 min at 60% B, 35-45 min at 96% B, 45.1-60
786 min at 60% B. The Nanospray Flex Ion Source (ThermoFisher Scientific) provided with a
787 stainless steel emitter was used to generate positively charged ions at 2.2 kV spray voltage.
788 Precursor ions were measured in full scan mode within a mass range of m/z 300-1600 at a
789 resolution of 70k FWHM using a maximum injection time of 120 ms and an automatic gain
790 control target of 1e6. For data-dependent acquisition, up to 10 most abundant precursor ions
791 per scan cycle with an assigned charge state of z = 2-6 were selected in the quadrupole for
792 further fragmentation using an isolation width of m/z 2.0. Fragment ions were generated in
793 the HCD cell at a normalised collision energy of 30 V using nitrogen gas. Dynamic exclusion
794 of precursor ions was set to 20 s. Fragment ions were monitored at a resolution of 17.5k
795 (FWHM) using a maximum injection time of 120 ms and an AGC target of 2e5.

796

797 **Protein database search**

798 Thermo raw files were processed by the Proteome Discoverer (PD) software v1.4.0.288
799 (Thermo). Tandem mass spectra were searched against the *Candida* Genome Database
800 (http://www.candidagenome.org/download/sequence/C_albicans_SC5314/Assembly22/current/C_albicans_SC5314_A22_current_orf_trans_all.fasta.gz; status: 2015/05/03) using the
801 Sequest HT search algorithm. Mass spectra were searched for both unspecific cleavages (no
802 enzyme) and tryptic peptides with up to 4 missed cleavages. The precursor mass tolerance
803

804 was set to 10 ppm and the fragment mass tolerance to 0.02 Da. Target Decoy PSM Validator
805 node and a reverse decoy database was used for (qvalue) validation of the peptide spectral
806 matches (PSMs) using a strict target false discovery (FDR) rate of < 1%. Furthermore, we
807 used the Score versus Charge State function of the Sequest engine to filter out insignificant
808 peptide hits (xcorr of 2.0 for z=2, 2.25 for z=3, 2.5 for z=4, 2.75 for z=5, 3.0 for z=6). At
809 least two unique peptides per protein were required for positive protein hits.

810

811 **Statistics**

812 TransAM and patch clamp data were analyzed using a paired t-test whilst cytokines, LDH
813 and calcium influx data were analyzed using one-way ANOVA with all compared groups
814 passing an equal variance test. Murine *in vivo* data was analyzed using the Mann-Whitney
815 test. Zebrafish data was analyzed using the Kruskal-Wallis test with Dunn's multiple
816 comparison correction. In all cases, $P < 0.05$ was taken to be significant.

817

818 32 Rupniak, H. T. *et al.* Characteristics of four new human cell lines derived from
819 squamous cell carcinomas of the head and neck. *J Natl Cancer Inst* **75**, 621-635
820 (1985).

821 33 Mayer, F. L. *et al.* The novel *Candida albicans* transporter Dur31 Is a multi-stage
822 pathogenicity factor. *PLoS pathog* **8**, e1002592 (2012).

823 34 Gillum, A. M., Tsay, E. Y. & Kirsch, D. R. Isolation of the *Candida albicans* gene for
824 orotidine-5'-phosphate decarboxylase by complementation of *S. cerevisiae* *ura3* and
825 *E. coli* *pyrF* mutations. *Mol Gen Genet* **198**, 179-182 (1984).

826 35 Citiulo, F. *et al.* *Candida albicans* scavenges host zinc via Pra1 during endothelial
827 invasion. *PLoS pathog* **8**, e1002777 (2012).

828 36 Gola, S., Martin, R., Walther, A., Dunkler, A. & Wendland, J. New modules for PCR-
829 based gene targeting in *Candida albicans*: rapid and efficient gene targeting using 100
830 bp of flanking homology region. *Yeast* **20**, 1339-1347 (2003).

831 37 Wilson, R. B., Davis, D. & Mitchell, A. P. Rapid hypothesis testing with *Candida*
832 *albicans* through gene disruption with short homology regions. *J Bacteriol* **181**, 1868-
833 1874 (1999).

834 38 Walther, A. & Wendland, J. An improved transformation protocol for the human
835 fungal pathogen *Candida albicans*. *Curr Genet* **42**, 339-343 (2003).

836 39 Murad, A. M., Lee, P. R., Broadbent, I. D., Barelle, C. J. & Brown, A. J. Clp10, an
837 efficient and convenient integrating vector for *Candida albicans*. *Yeast* **16**, 325-327
838 (2000).

839 40 Gratacap, R. L., Rawls, J. F. & Wheeler, R. T. Mucosal candidiasis elicits NF-kappaB
840 activation, proinflammatory gene expression and localized neutrophilia in zebrafish.
841 *Dis Model Mech* **6**, 1260-1270 (2013).

842 41 Moyes, D. L. *et al.* A biphasic innate immune MAPK response discriminates between
843 the yeast and hyphal forms of *Candida albicans* in epithelial cells. *Cell Host Microbe*
844 **8**, 225-235 (2010).

845 42 Moyes, D. L. *et al.* *Candida albicans* yeast and hyphae are discriminated by MAPK
846 signaling in vaginal epithelial cells. *PloS ONE* **6**, e26580 (2011).

847 43 Wachtler, B., Wilson, D., Haedicke, K., Dalle, F. & Hube, B. From attachment to
848 damage: defined genes of *Candida albicans* mediate adhesion, invasion and damage
849 during interaction with oral epithelial cells. *PloS ONE* **6**, e17046 (2011).

850 44 Trinh le, A. *et al.* A versatile gene trap to visualize and interrogate the function of the
851 vertebrate proteome. *Gene Devel* **25**, 2306-2320 (2011).

852 45 Solis, N. V. & Filler, S. G. Mouse model of oropharyngeal candidiasis. *Nat Protoc* **7**,
853 637-642 (2012).

854 46 Cranfield, C., Carne, S., Martinac, B. & Cornell, B. The assembly and use of tethered
855 bilayer lipid membranes (tBLMs). *Methods Mol Biol* **1232**, 45-53 (2015).

856 47 Cranfield, C. G. *et al.* Transient potential gradients and impedance measures of
857 tethered bilayer lipid membranes: pore-forming peptide insertion and the effect of
858 electroporation. *Biophys J* **106**, 182-189 (2014).

859 48 Schromm, A. B. *et al.* Lipopolysaccharide-binding protein mediates CD14-
860 independent intercalation of lipopolysaccharide into phospholipid membranes. *FEBS*
861 *Lett* **399**, 267-271 (1996).

862 49 Chen, G. C. & Yang, J. T. 2-Point Calibration of Circular Dichrometer with D-10-
863 Camphorsulfonic Acid. *Anal. Lett* **10**, 1195-1207 (1977).

864 50 Montal, M. & Mueller, P. Formation of bimolecular membranes from lipid
865 monolayers and a study of their electrical properties. *Proc Natl Acad Sci U S A* **69**,
866 3561-3566 (1972).

867 51 Gutschmann, T., Heimburg, T., Keyser, U., Mahendran, K. R. & Winterhalter, M.
868 Protein reconstitution into freestanding planar lipid membranes for
869 electrophysiological characterization. *Nat Protoc* **10**, 188-198 (2015).

870

871 **Extended Data Table references:**

- 872 52 Gillum, A. M., Tsay, E. Y. & Kirsch, D. R. Isolation of the *Candida albicans* gene for
873 orotidine-5'-phosphate decarboxylase by complementation of *S. cerevisiae* *ura3* and
874 *E. coli* *pyrF* mutations. *Mol Gen Genet* **198**, 179-182 (1984).
- 875 53 Wilson, R. B., Davis, D. & Mitchell, A. P. Rapid hypothesis testing with *Candida*
876 *albicans* through gene disruption with short homology regions. *J Bacteriol* **181**, 1868-
877 1874 (1999).
- 878 54 Fonzi, W. A. & Irwin, M. Y. Isogenic strain construction and gene mapping in
879 *Candida albicans*. *Genetics* **134**, 717-728 (1993).
- 880 55 Davis, D., Wilson, R. B. & Mitchell, A. P. *RIM101*-dependent and-independent
881 pathways govern pH responses in *Candida albicans*. *Mol Cell Biol* **20**, 971-978
882 (2000).
- 883 56 Braun, B. R. & Johnson, A. D. TUP1, CPH1 and EFG1 make independent
884 contributions to filamentation in *Candida albicans*. *Genetics* **155**, 57-67 (2000).
- 885 57 Lo, H. J. *et al.* Nonfilamentous *C. albicans* mutants are avirulent. *Cell* **90**, 939-949
886 (1997).
- 887 58 Moyes, D. L. *et al.* A biphasic innate immune MAPK response discriminates between
888 the yeast and hyphal forms of *Candida albicans* in epithelial cells. *Cell Host Microbe*
889 **8**, 225-235 (2010).
- 890 59 Zakikhany, K. *et al.* In vivo transcript profiling of *Candida albicans* identifies a gene
891 essential for interepithelial dissemination. *Cell Microbiol* **9**, 2938-2954 (2007).
- 892 60 Cao, F. *et al.* The Flo8 transcription factor is essential for hyphal development and
893 virulence in *Candida albicans*. *Mol Biol Cell* **17**, 295-307 (2006).
- 894 61 Bockmuhl, D. P., Krishnamurthy, S., Gerads, M., Sonneborn, A. & Ernst, J. F.
895 Distinct and redundant roles of the two protein kinase A isoforms Tpk1p and Tpk2p
896 in morphogenesis and growth of *Candida albicans*. *Mol Microbiol* **42**, 1243-1257
897 (2001).
- 898 62 Sonneborn, A. *et al.* Protein kinase A encoded by TPK2 regulates dimorphism of
899 *Candida albicans*. *Mol Microbiol* **35**, 386-396 (2000).
- 900 63 Palmer, G. E., Cashmore, A. & Sturtevant, J. *Candida albicans* *VPS11* is required for
901 vacuole biogenesis and germ tube formation. *Eukaryot Cell* **2**, 411-421 (2003).

902 64 Zou, H., Fang, H. M., Zhu, Y. & Wang, Y. *Candida albicans* Cyr1, Cap1 and G-actin
903 form a sensor/effector apparatus for activating cAMP synthesis in hyphal growth. *Mol*
904 *Microbiol* **75**, 579-591 (2010).

905 65 Bates, S. *et al.* Outer chain N-glycans are required for cell wall integrity and virulence
906 of *Candida albicans*. *J Biol Chem* **281**, 90-98 (2006).

907 66 Murciano, C. *et al.* *Candida albicans* cell wall glycosylation may be indirectly
908 required for activation of epithelial cell proinflammatory responses. *Infect Immun* **79**,
909 4902-4911 (2011).

910 67 Newport, G. & Agabian, N. *KEX2* influences *Candida albicans* proteinase secretion
911 and hyphal formation. *J Biol Chem* **272**, 28954-28961 (1997).

912 68 Murad, A. M. *et al.* *NRG1* represses yeast-hypha morphogenesis and hypha-specific
913 gene expression in *Candida albicans*. *EMBO J* **20**, 4742-4752 (2001).

914 69 Liu, H., Kohler, J. & Fink, G. R. Suppression of hyphal formation in *Candida*
915 *albicans* by mutation of a *STE12* homolog. *Science* **266**, 1723-1726 (1994).

916 70 Lane, S., Zhou, S., Pan, T., Dai, Q. & Liu, H. The basic helix-loop-helix transcription
917 factor Cph2 regulates hyphal development in *Candida albicans* partly via *TEC1*. *Mol*
918 *Cell Biol* **21**, 6418-6428 (2001).

919 71 White, S. J. *et al.* Self-regulation of *Candida albicans* population size during GI
920 colonization. *PLoS pathog* **3**, e184 (2007).

921 72 Brown, D. H., Jr., Giusani, A. D., Chen, X. & Kumamoto, C. A. Filamentous growth
922 of *Candida albicans* in response to physical environmental cues and its regulation by
923 the unique *CZF1* gene. *Mol Microbiol* **34**, 651-662 (1999).

924 73 Kadosh, D. & Johnson, A. D. Rfg1, a protein related to the *Saccharomyces cerevisiae*
925 hypoxic regulator Rox1, controls filamentous growth and virulence in *Candida*
926 *albicans*. *Mol Cell Biol* **21**, 2496-2505 (2001).

927 74 San Jose, C., Monge, R. A., Perez-Diaz, R., Pla, J. & Nombela, C. The mitogen-
928 activated protein kinase homolog *HOG1* gene controls glycerol accumulation in the
929 pathogenic fungus *Candida albicans*. *J Bacteriol* **178**, 5850-5852 (1996).

930 75 Firon, A. *et al.* The *SUN41* and *SUN42* genes are essential for cell separation in
931 *Candida albicans*. *Mol Microbiol* **66**, 1256-1275 (2007).

932 76 de Boer, A. D. *et al.* The *Candida albicans* cell wall protein Rhd3/Pga29 is abundant
933 in the yeast form and contributes to virulence. *Yeast* **27**, 611-624 (2010).

934 77 Muhlschlegel, F. A. & Fonzi, W. A. *PHR2* of *Candida albicans* encodes a functional
935 homolog of the pH-regulated gene *PHR1* with an inverted pattern of pH-dependent
936 expression. *Mol Cell Biol* **17**, 5960-5967 (1997).

937 78 Martin, R. *et al.* A core filamentation response network in *Candida albicans* is
938 restricted to eight genes. *PLoS ONE* **8**, e58613 (2013).

939 79 Birse, C. E., Irwin, M. Y., Fonzi, W. A. & Sypherd, P. S. Cloning and
940 characterization of *ECE1*, a gene expressed in association with cell elongation of the
941 dimorphic pathogen *Candida albicans*. *Infect Immun* **61**, 3648-3655 (1993).

942 80 Navarro-Garcia, F., Sanchez, M., Pla, J. & Nombela, C. Functional characterization of
943 the *MKCl* gene of *Candida albicans*, which encodes a mitogen-activated protein
944 kinase homolog related to cell integrity. *Mol Cell Biol* **15**, 2197-2206 (1995).

945 81 Hausauer, D. L., Gerami-Nejad, M., Kistler-Anderson, C. & Gale, C. A. Hyphal
946 guidance and invasive growth in *Candida albicans* require the Ras-like GTPase Rsr1p
947 and its GTPase-activating protein Bud2p. *Eukaryot Cell* **4**, 1273-1286 (2005).

948 82 Sentandreu, M., Elorza, M. V., Sentandreu, R. & Fonzi, W. A. Cloning and
949 characterization of *PRA1*, a gene encoding a novel pH-regulated antigen of *Candida*
950 *albicans*. *J Bacteriol* **180**, 282-289 (1998).

951 83 Pardini, G. *et al.* The *CRH* family coding for cell wall glycosylphosphatidylinositol
952 proteins with a predicted transglycosidase domain affects cell wall organization and
953 virulence of *Candida albicans*. *J Biol Chem* **281**, 40399-40411 (2006).

954 84 Braun, B. R., Head, W. S., Wang, M. X. & Johnson, A. D. Identification and
955 characterization of *TUPI*-regulated genes in *Candida albicans*. *Genetics* **156**, 31-44
956 (2000).

957 85 Fradin, C. *et al.* Granulocytes govern the transcriptional response, morphology and
958 proliferation of *Candida albicans* in human blood. *Mol Microbiol* **56**, 397-415 (2005).

959 86 Staab, J. F., Bradway, S. D., Fidel, P. L. & Sundstrom, P. Adhesive and mammalian
960 transglutaminase substrate properties of *Candida albicans* Hwp1. *Science* **283**, 1535-
961 1538 (1999).

962 87 Bailey, D. A., Feldmann, P. J., Bovey, M., Gow, N. A. & Brown, A. J. The *Candida*
963 *albicans* *HYR1* gene, which is activated in response to hyphal development, belongs
964 to a gene family encoding yeast cell wall proteins. *J Bacteriol* **178**, 5353-5360 (1996).

965 88 Sandini, S., La Valle, R., De Bernardis, F., Macri, C. & Cassone, A. The 65 kDa
966 mannoprotein gene of *Candida albicans* encodes a putative beta-glucanase adhesin

967 required for hyphal morphogenesis and experimental pathogenicity. *Cell Microbiol* **9**,
968 1223-1238 (2007).

969 89 Csank, C. *et al.* Roles of the *Candida albicans* mitogen-activated protein kinase
970 homolog, Cek1p, in hyphal development and systemic candidiasis. *Infect Immun* **66**,
971 2713-2721 (1998).

972 90 Hube, B. *et al.* Disruption of each of the secreted aspartyl proteinase genes *SAP1*,
973 *SAP2*, and *SAP3* of *Candida albicans* attenuates virulence. *Infect Immun* **65**, 3529-
974 3538 (1997).

975 91 Taylor, B. N. *et al.* Induction of *SAP7* correlates with virulence in an intravenous
976 infection model of candidiasis but not in a vaginal infection model in mice. *Infect*
977 *Immun* **73**, 7061-7063 (2005).

978 92 Schild, L. *et al.* Proteolytic cleavage of covalently linked cell wall proteins by
979 *Candida albicans* Sap9 and Sap10. *Eukaryot Cell* **10**, 98-109 (2011).

980 93 Zhao, X. *et al.* *ALS3* and *ALS8* represent a single locus that encodes a *Candida*
981 *albicans* adhesin; functional comparisons between Als3p and Als1p. *Microbiol* **150**,
982 2415-2428 (2004).

983 94 Murciano, C. *et al.* Evaluation of the role of *Candida albicans* agglutinin-like
984 sequence (Als) proteins in human oral epithelial cell interactions. *PloS ONE* **7**,
985 e33362 (2012).

986 95 Zhao, X., Oh, S. H., Yeater, K. M. & Hoyer, L. L. Analysis of the *Candida albicans*
987 Als2p and Als4p adhesins suggests the potential for compensatory function within the
988 Als family. *Microbiol* **151**, 1619-1630 (2005).

989 96 Zhao, X., Oh, S. H. & Hoyer, L. L. Deletion of *ALS5*, *ALS6* or *ALS7* increases
990 adhesion of *Candida albicans* to human vascular endothelial and buccal epithelial
991 cells. *Med Mycol* **45**, 429-434 (2007).

992 97 Zhao, X., Oh, S. H. & Hoyer, L. L. Unequal contribution of *ALS9* alleles to adhesion
993 between *Candida albicans* and human vascular endothelial cells. *Microbiol* **153**,
994 2342-2350 (2007).

995 98 Timpel, C., Strahl-Bolsinger, S., Ziegelbauer, K. & Ernst, J. F. Multiple functions of
996 Pmt1p-mediated protein O-mannosylation in the fungal pathogen *Candida albicans*. *J*
997 *Biol Chem* **273**, 20837-20846 (1998).

998 99 Bates, S. *et al.* *Candida albicans* Pmr1p, a secretory pathway P-type Ca²⁺/Mn²⁺-
999 ATPase, is required for glycosylation and virulence. *J Biol Chem* **280**, 23408-23415
1000 (2005).

1001 100 Hobson, R. P. *et al.* Loss of cell wall mannosylphosphate in *Candida albicans* does
1002 not influence macrophage recognition. *J Biol Chem* **279**, 39628-39635 (2004).

1003 101 Southard, S. B., Specht, C. A., Mishra, C., Chen-Weiner, J. & Robbins, P. W.
1004 Molecular analysis of the *Candida albicans* homolog of *Saccharomyces cerevisiae*
1005 *MNN9*, required for glycosylation of cell wall mannoproteins. *J Bacteriol* **181**, 7439-
1006 7448 (1999).

1007 102 Munro, C. A. *et al.* Mnt1p and Mnt2p of *Candida albicans* are partially redundant
1008 alpha-1,2-mannosyltransferases that participate in O-linked mannosylation and are
1009 required for adhesion and virulence. *J Biol Chem* **280**, 1051-1060 (2005).

1010 103 Mio, T. *et al.* Role of three chitin synthase genes in the growth of *Candida albicans*. *J*
1011 *Bacteriol* **178**, 2416-2419 (1996).

1012 104 Mille, C. *et al.* Inactivation of *CaMIT1* inhibits *Candida albicans* phospholipomannan
1013 beta-mannosylation, reduces virulence, and alters cell wall protein beta-
1014 mannosylation. *J Biol Chem* **279**, 47952-47960 (2004).

1015 105 Mille, C. *et al.* Identification of a new family of genes involved in beta-1,2-
1016 mannosylation of glycans in *Pichia pastoris* and *Candida albicans*. *J Biol Chem* **283**,
1017 9724-9736 (2008).

1018 106 Mille, C. *et al.* Members 5 and 6 of the *Candida albicans* *BMT* family encode
1019 enzymes acting specifically on beta-mannosylation of the phospholipomannan cell-
1020 wall glycosphingolipid. *Glycobiol* **22**, 1332-1342 (2012).

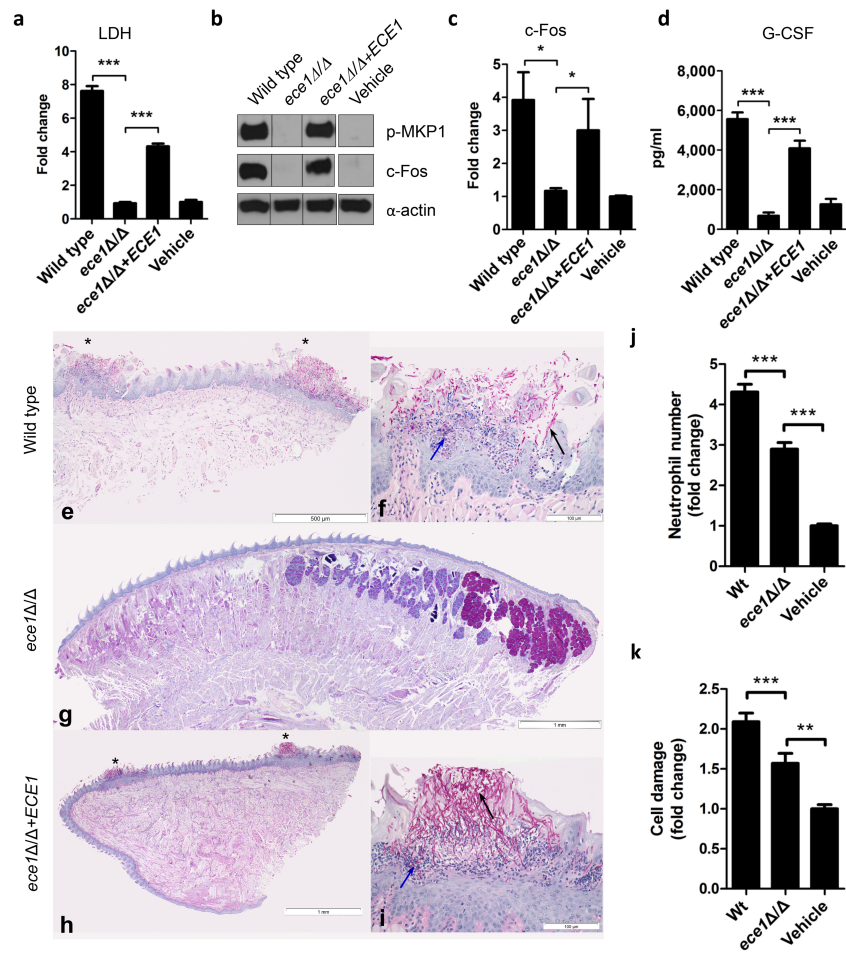
1021 107 Mio, T. *et al.* Cloning of the *Candida albicans* homolog of *Saccharomyces cerevisiae*
1022 *GSCI/FKS1* and its involvement in beta-1,3-glucan synthesis. *J Bacteriol* **179**, 4096-
1023 4105 (1997).

1024 108 Mio, T. *et al.* Isolation of the *Candida albicans* homologs of *Saccharomyces*
1025 *cerevisiae* *KRE6* and *SKN1*: expression and physiological function. *J Bacteriol* **179**,
1026 2363-2372 (1997).

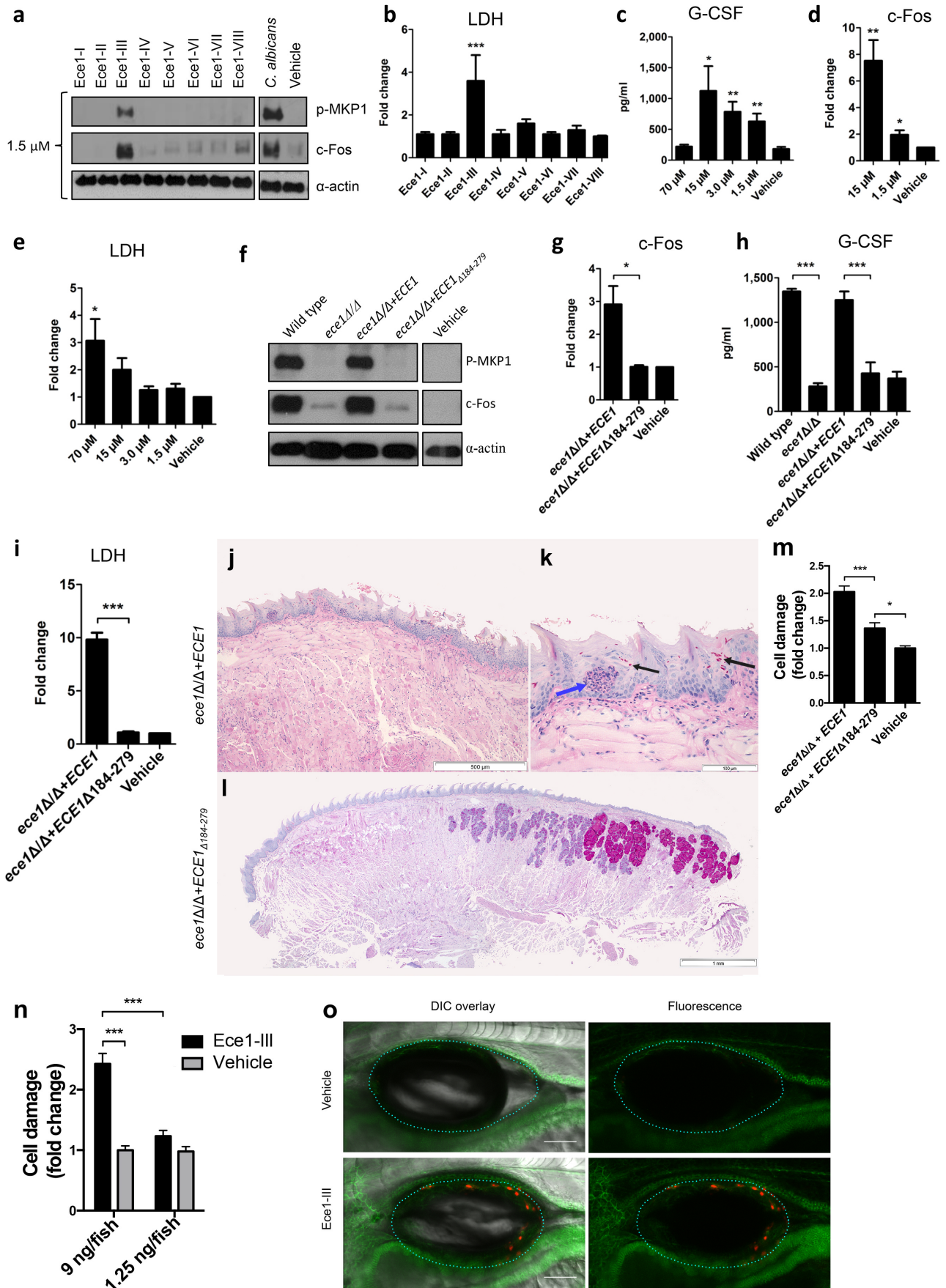
1027 109 Staab, J. F. & Sundstrom, P. *URA3* as a selectable marker for disruption and virulence
1028 assessment of *Candida albicans* genes. *Trends Microbiol* **11**, 69-73 (2003).

1029 110 Murad, A. M., Lee, P. R., Broadbent, I. D., Barelle, C. J. & Brown, A. J. Clp10, an
1030 efficient and convenient integrating vector for *Candida albicans*. *Yeast* **16**, 325-327
1031 (2000).

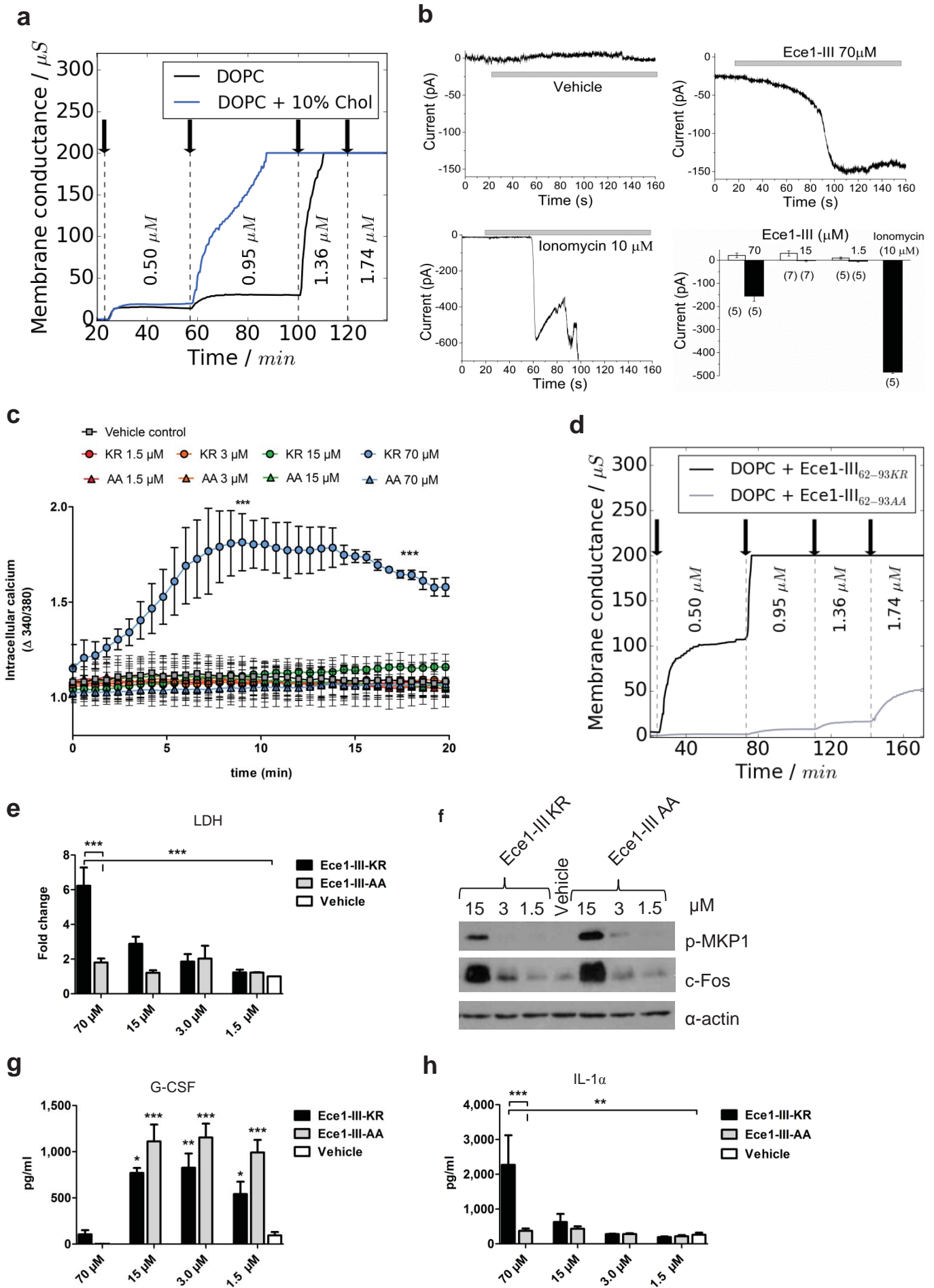
1032

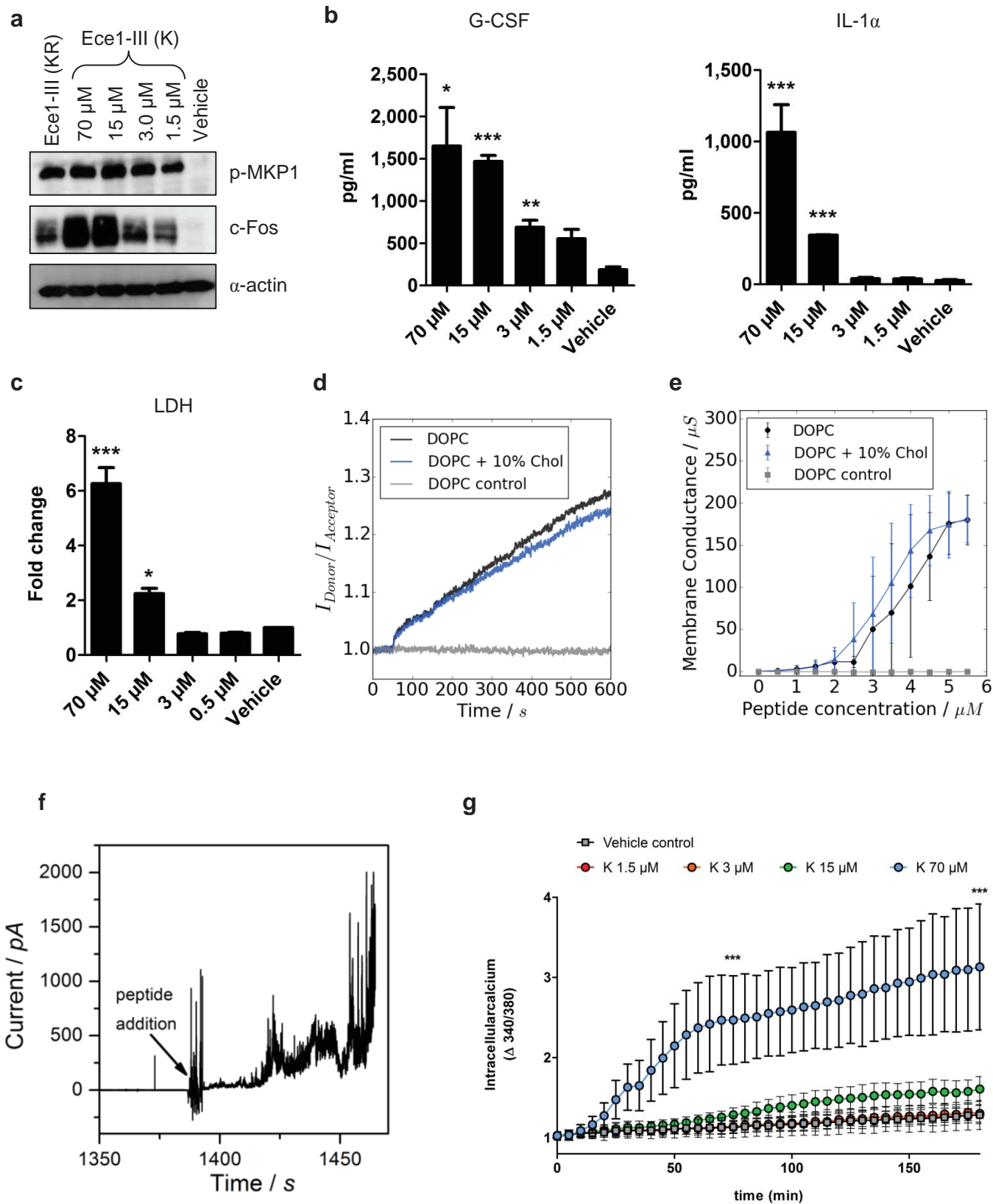


Hube_Figure 1

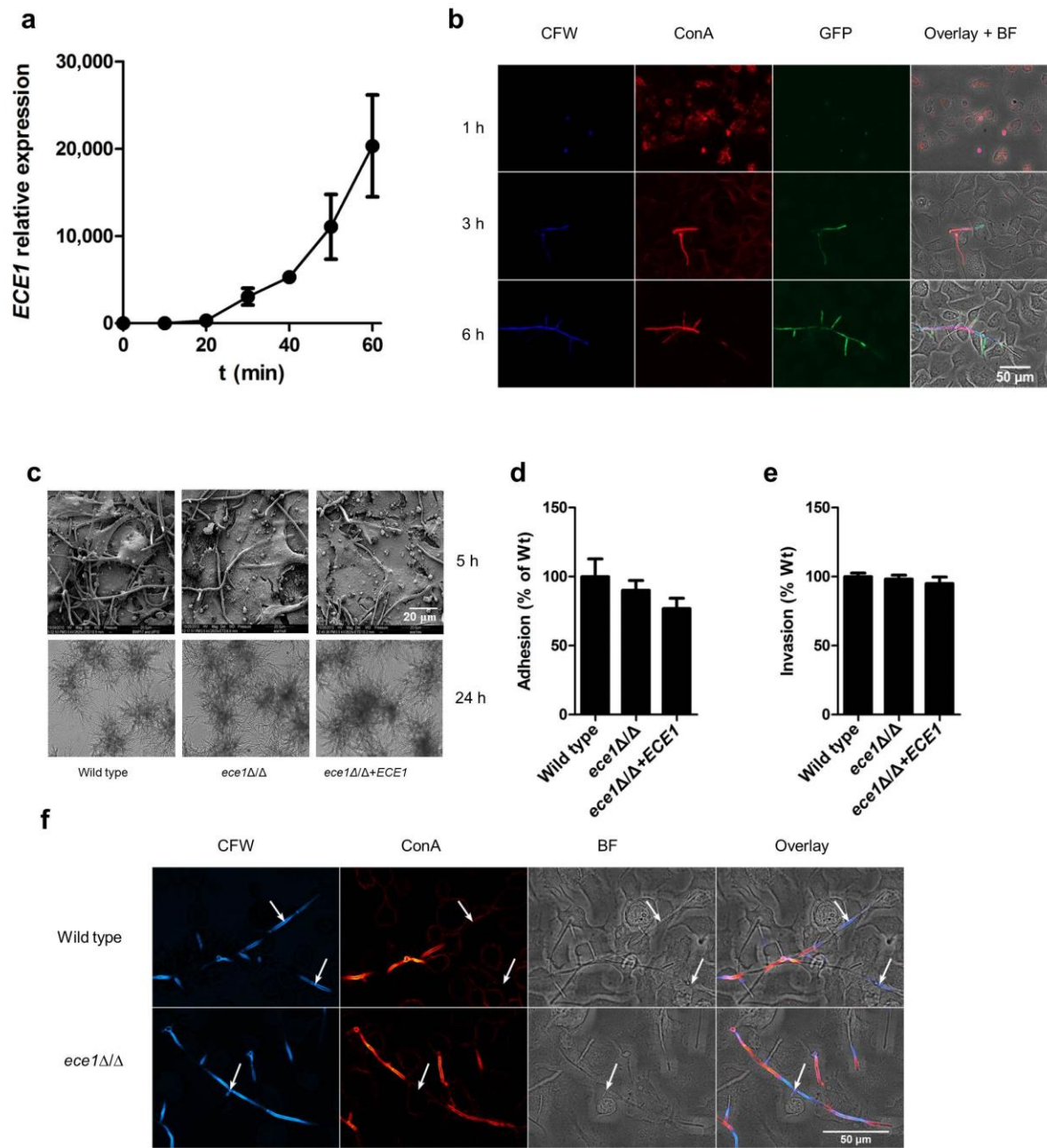


Hube_Figure 2

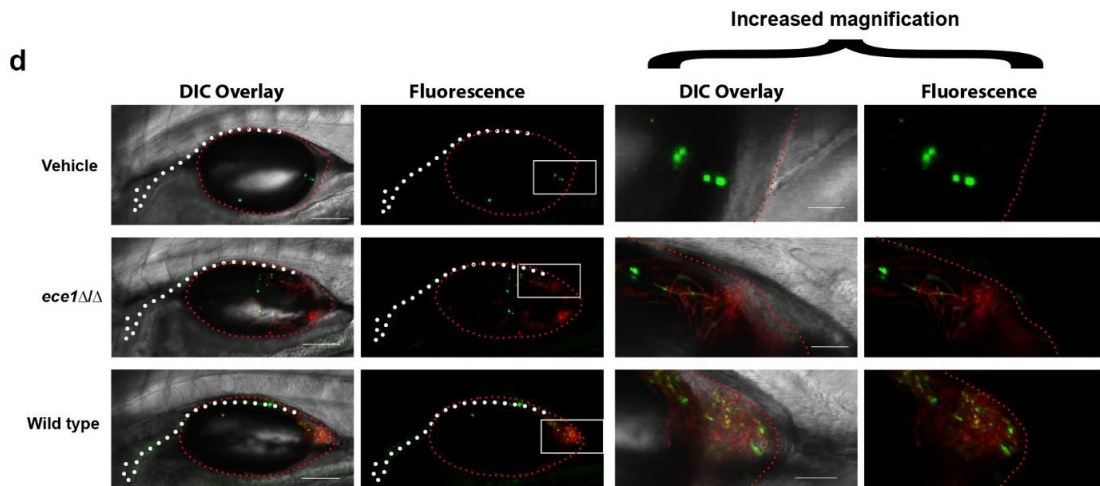
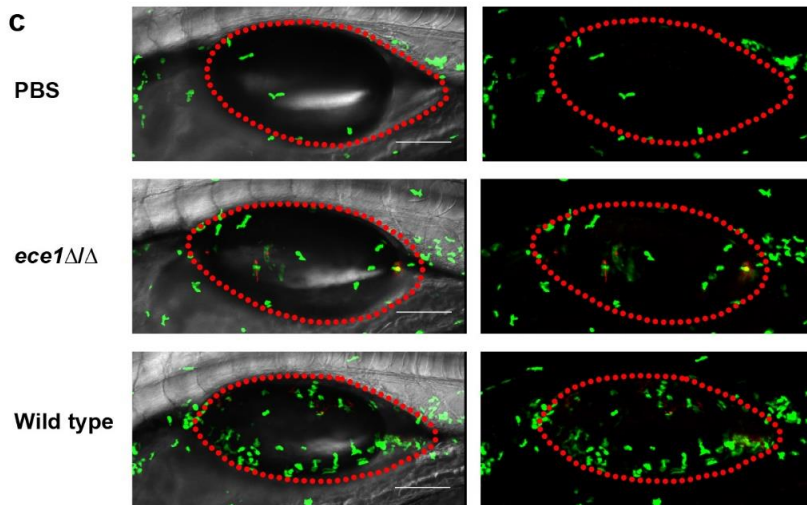
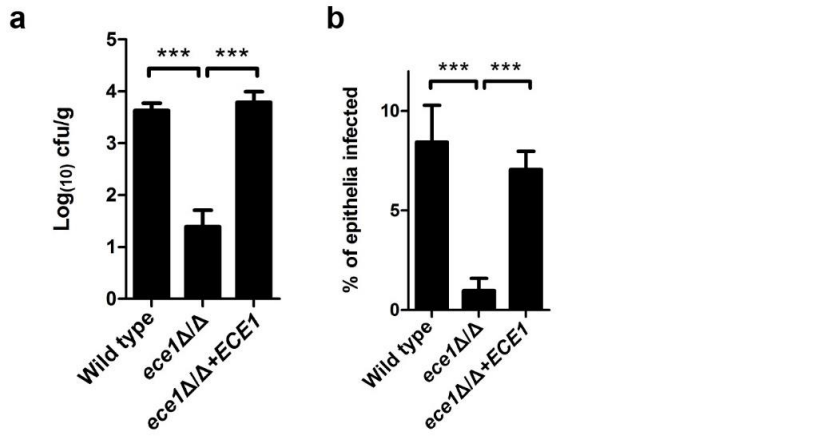




Hube_Figure 4



Extended Figure 1



Extended Figure 2

a

***Candida albicans* Ece1p amino acid sequence:**

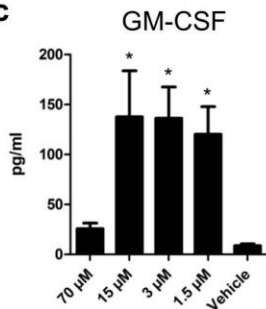
MKFSKIACATVFALSSQAAIIHHAPEFNMKR DVAPAAPAAPADQAPTVPAPQEFNTAITKR SIIIGIIMGILGNIPQVIQIIMSIVKAFKGNKREIDIDSVVAGI IADMPFVVRVADTAMTSVASTKRDGANDDVANAVVRLPEIVARVATGVQOSIENAKRDGVPDVLGNLVANAPRLISNVFDGVSETVQQA KR DGLDFLDELQRLPQLITRSAESALKDSQPVKR DAGSVALSNLIKKS IETVGIENAAQIVSERDISLIEEYFGKA



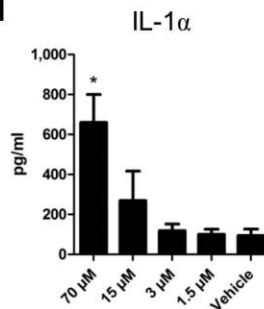
b

Ece1-I₁₋₃₁ MKFSKIACATVFALSSQAAIIHHAPEFNMKR
 Ece1-II₃₂₋₆₁ DVAPAAPAAPADQAPTVPAPQEFNTAITKR
 Ece1-III₆₂₋₉₃ SIIIGIIMGILGNIPQVIQIIMSIVKAFKGNKR
 Ece1-IV₉₄₋₁₂₆ EDIDSVVAGI IADMPFVVRVADTAMTSVASTKR
 Ece1-V₁₂₇₋₁₆₀ DGANDDVANAVVRLPEIVARVATGVQOSIENAKR
 Ece1-VI₁₆₁₋₁₉₄ DGVPDVLGNLVANAPRLISNVFDGVSETVQQA KR
 Ece1-VII₁₉₅₋₂₂₈ DGLDFLDELQRLPQLITRSAESALKDSQPVKR
 Ece1-VIII₂₂₉₋₂₇₁ DAGSVALSNLIKKS IETVGIENAAQIVSERDISLIEEYFGKA

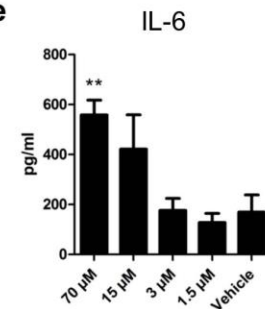
c



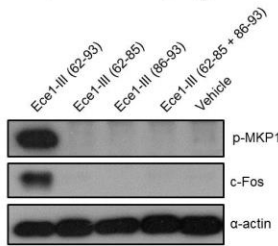
d



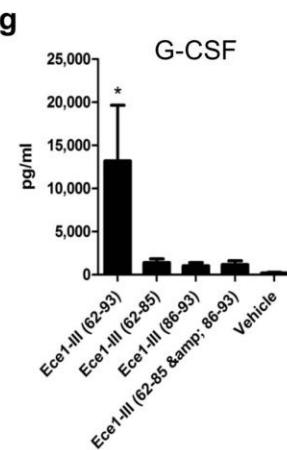
e



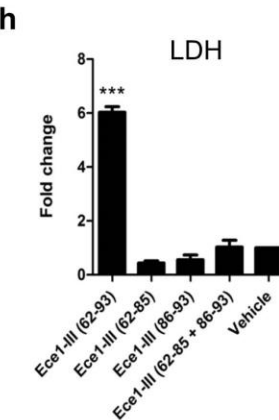
f



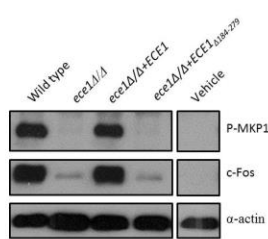
g



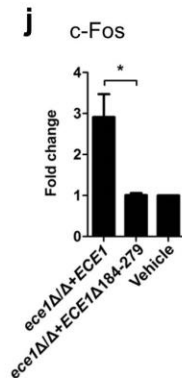
h



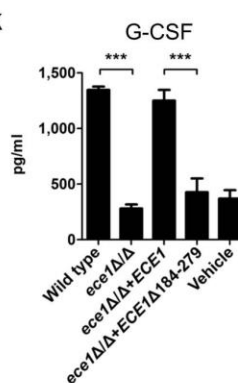
i



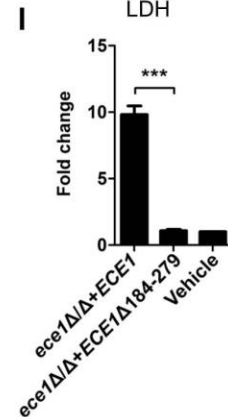
j



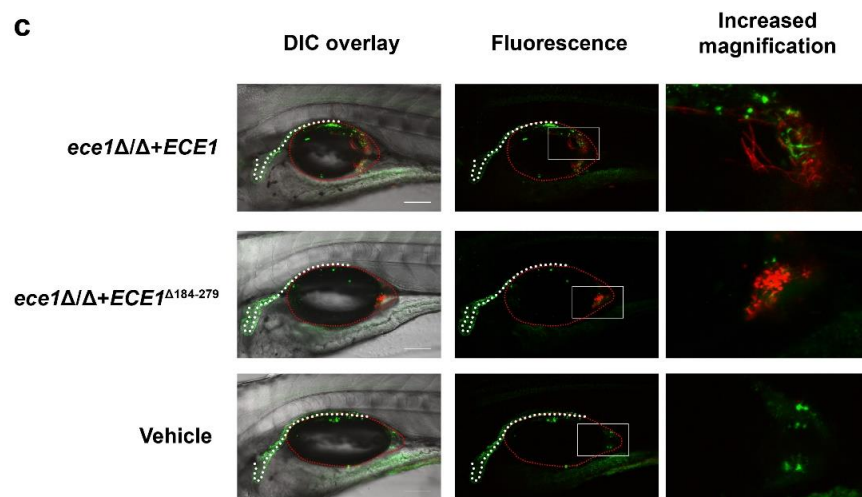
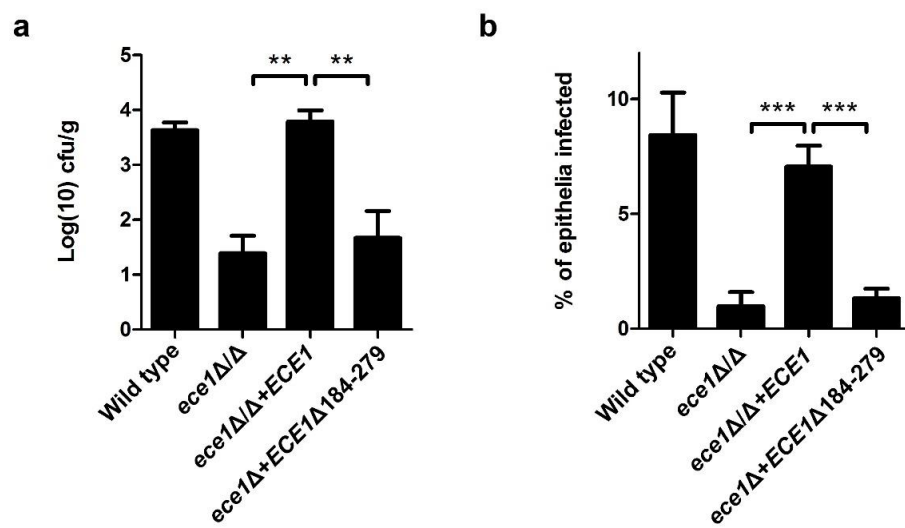
k



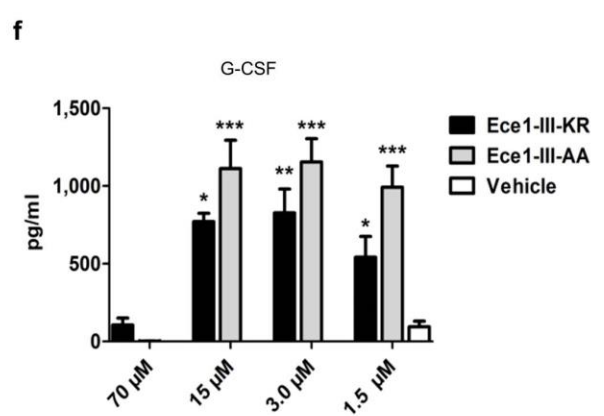
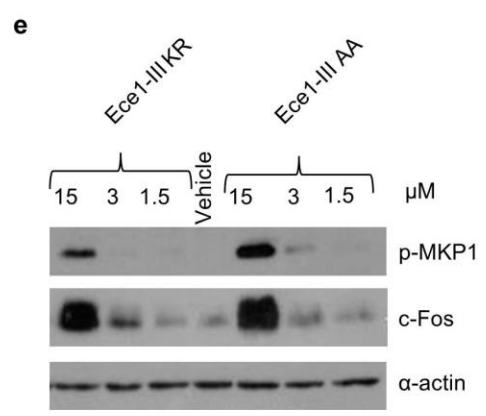
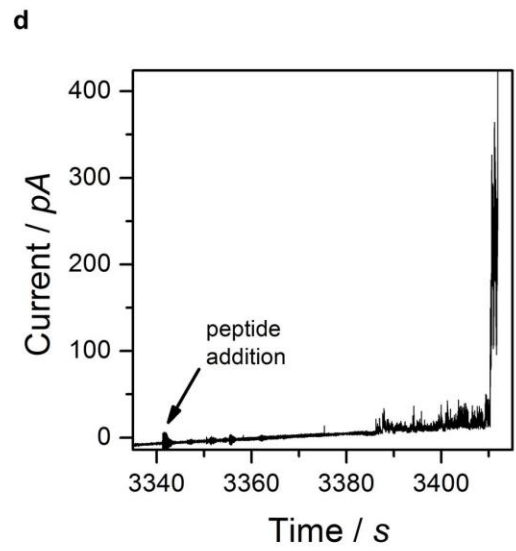
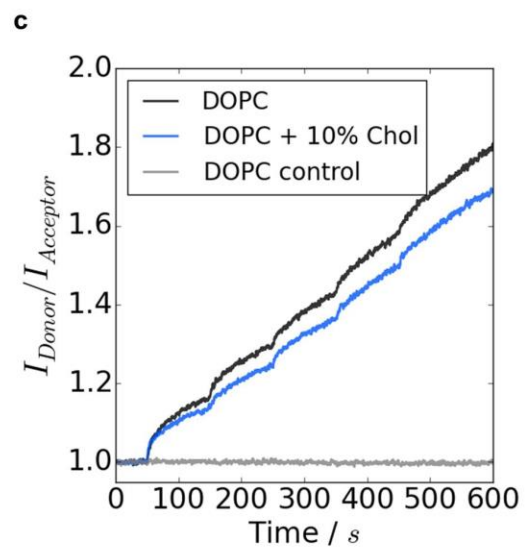
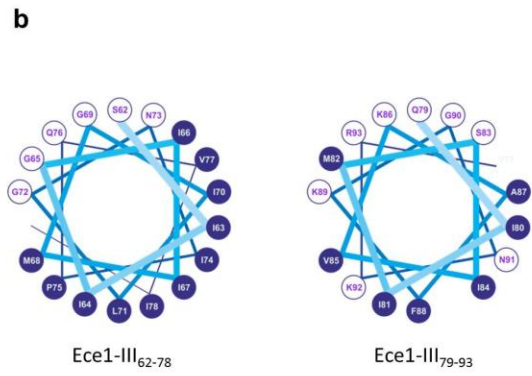
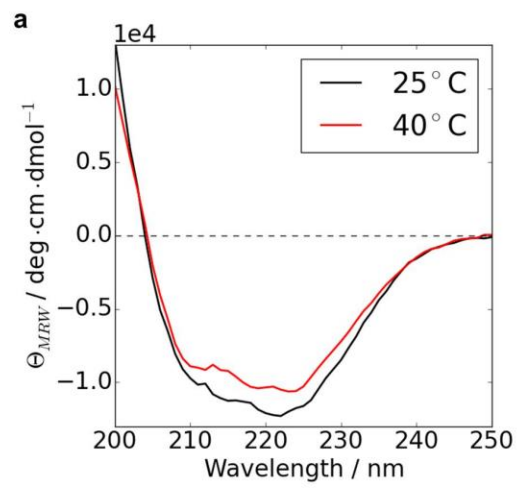
l



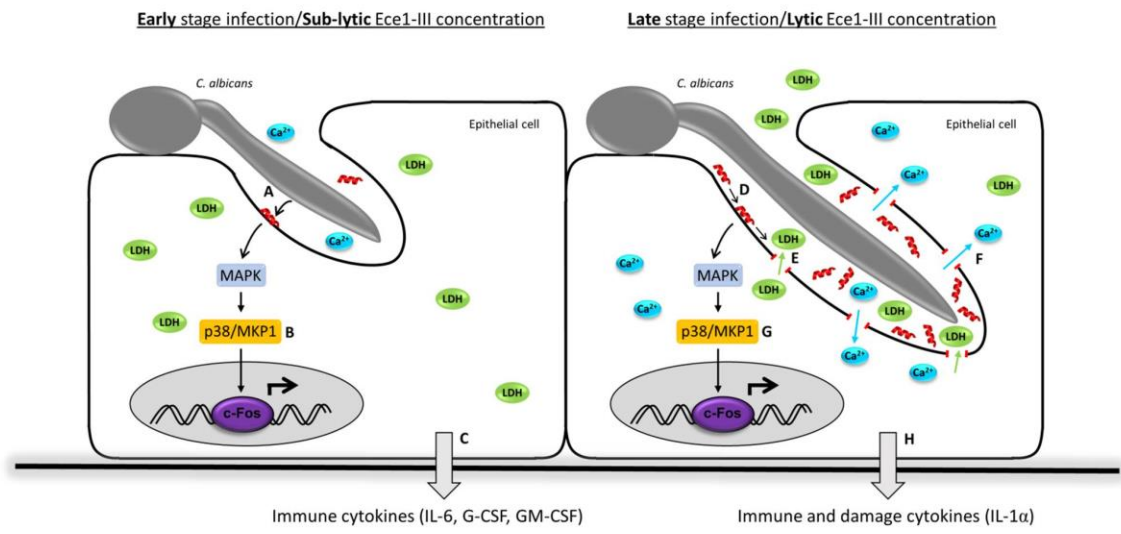
Extended Figure 3



Extended Figure 4



Extended Figure 5



Extended Figure 6

Extended Data Table 1. *C. albicans* strains used in this study.

Strain name	Strain/Gene Function	Strain Reference	Morphology [†]	Phospho-MKP1 [†]	c-Fos [†]	Cytokines [‡]	Damage [§]	Phenotype Reference
Controls								
SC5314	Wild type	[52]	Hyphae	Yes	Yes	Yes	Yes	This study
BWP17 & Clp30	Parental strain	[53]	Hyphae	Yes	Yes	Yes	Yes	This study
CAI-4 & Clp10	Parental strain	[54]	Hyphae	Yes	Yes	Yes	Yes	This study
CAF2-1	Parental strain	[54]	Hyphae	Yes	Yes	Yes	Yes	This study
DAY286	Parental strain	[55]	Hyphae	Yes	Yes	Yes	Yes	This study
Yeast-locked								
<i>efg1Δ/Δ</i>	Transcription factor	[56]	Yeast	No	No	No	No	This study
<i>efg1/cph1Δ/Δ</i>	Transcription factor/ Transcription factor	[57]	Yeast	No	No	No	No	[58]/This study
<i>eed1Δ/Δ</i>	RNA polymerase II regulator	[59]	Yeast	No	No	No	No	[58]/This study
<i>flo8Δ/Δ</i>	Transcription factor	[60]	Yeast	No	No	No	No	This study
<i>tpk1Δ/Δ</i>	cAMP-dependent protein kinase	[61]	Yeast	No	No	No	No	This study
<i>tpk2Δ/Δ</i>	cAMP-dependent protein kinase	[62]	Yeast	No	No	No	No	This study
<i>vps11Δ/Δ</i>	Protein trafficking	[63]	Yeast	No	No	No	No	This study
<i>cap1Δ/Δ</i>	Transcription factor	[64]	Yeast	No	No	Yes	No	This study
<i>och1Δ/Δ</i>	Alpha-1,6-mannosyltransferase	[65]	Yeast	No	No	No	No	[66]
<i>kex2Δ/Δ</i>	Processing enzyme	[67]	Yeast	No	No	No	No	This study
Hypha-producing								
<i>nrg1Δ/Δ</i>	Transcriptional corepressor	[68]	Hyphae	Yes	Yes	Yes	Yes	[58]/This study
<i>cph1Δ/Δ</i>	Transcription factor	[69]	Hyphae	Yes	Yes	Yes	Yes	This study
<i>cph2Δ/Δ</i>	Transcription factor	[70]	Hyphae	Yes	Yes	Yes	Yes	This study
<i>efh1Δ/Δ</i>	Transcription factor	[71]	Hyphae	Yes	Yes	Yes	Yes	This study
<i>czj1Δ/Δ</i>	Transcription factor	[72]	Hyphae	Yes	Yes	Yes	Yes	This study
<i>rfg1Δ/Δ</i>	Transcriptional repressor	[73]	Hyphae	Yes	Yes	Yes	Yes	This study
<i>hog1Δ/Δ</i>	MAP kinase	[74]	Hyphae	Yes	Yes	Yes	Yes	This study
<i>sun42Δ/Δ</i>	Adhesin-like protein	[75]	Hyphae	Yes	Yes	Yes	Yes	This study
<i>pga29Δ/Δ</i>	GPI-anchored yeast-associated protein	[76]	Hyphae	Yes	Yes	Yes	Yes	This study
<i>phr2Δ/Δ</i>	Glycosidase	[77]	Hyphae	Yes	Yes	Yes	Yes	This study
<i>pga36Δ/Δ</i>	GPI-anchored protein	[78]	Hyphae	Yes	Yes	Yes	Yes	This study
<i>ece1Δ/Δ</i>	Hypha-associated protein	[79]	Hyphae	No	No	No	No	This study
<i>mkk1Δ/Δ</i>	MAP kinase	[80]	Hyphae	Yes	Yes	Yes	Yes	This study
<i>bud2Δ/Δ</i>	GTPase activating protein	[81]	Hyphae	Yes	Yes	Yes	Yes	This study
<i>pra1Δ/Δ</i>	Zinc binding protein	[82]	Hyphae	Yes	Yes	Yes	Yes	This study
<i>utr2/crh11/crh12Δ/Δ</i>	Putative wall glycosidase/transglycosylase	[83]	Hyphae	Yes	Yes	Yes	Yes	This study
<i>wop1Δ/Δ</i>	Surface antigen on hyphae/buds	[84]	Hyphae	Yes	Yes	Yes	Yes	This study
<i>sod5Δ/Δ</i>	Superoxide dismutase	[85]	Hyphae	Yes	Yes	Yes	Yes	This study
<i>hwp1Δ/Δ</i>	Adhesin	[86]	Hyphae	Yes	Yes	Yes	Yes	This study
<i>rbt1Δ/Δ</i>	Putative GPI-modified cell wall protein	[84]	Hyphae	Yes	Yes	Yes	Yes	This study
<i>rbt5Δ/Δ</i>	Heme binding	[84]	Hyphae	Yes	Yes	Yes	Yes	This study
<i>hyr1Δ/Δ</i>	GPI anchored hyphal cell wall protein	[87]	Hyphae	Yes	Yes	Yes	Yes	This study
<i>mp65Δ/Δ</i>	Cell surface mannoprotein	[88]	Hyphae	Yes	Yes	Yes	Yes	This study
<i>cek1Δ/Δ</i>	ERK family protein kinase	[89]	Hyphae	Yes	Yes	Yes	Yes	This study
<i>sap2Δ/Δ</i>	Secreted aspartyl protease	[90]	Hyphae	Yes	Yes	Yes	Yes	This study
<i>sap7Δ/Δ</i>	Secreted aspartyl protease	[91]	Hyphae	Yes	Yes	Yes	Yes	This study
<i>sap9/sap10Δ/Δ</i>	Secreted aspartyl protease	[92]	Hyphae	Yes	Yes	Yes	Yes	This study
<i>als1Δ/Δ</i>	Agglutinin-like sequence protein	[93]	Hyphae	Yes	Yes	Yes	Yes	[94]
<i>als2Δ/Δ</i>	Agglutinin-like sequence protein	[95]	Hyphae	Yes	Yes	Yes	Yes	[94]
<i>als3Δ/Δ</i>	Adhesin	[93]	Hyphae	Yes	Yes	Partial [¶]	Partial [¶]	[94]
<i>als4Δ/Δ</i>	Agglutinin-like sequence protein	[95]	Hyphae	Yes	Yes	Yes	Yes	[94]
<i>als5Δ/Δ</i>	Agglutinin-like sequence protein	[96]	Hyphae	Yes	Yes	Yes	Yes	[94]
<i>als6Δ/Δ</i>	Agglutinin-like sequence protein	[96]	Hyphae	Yes	Yes	Yes	Yes	[94]
<i>als7Δ/Δ</i>	Agglutinin-like sequence protein	[96]	Hyphae	Yes	Yes	Yes	Yes	[94]
<i>als9Δ/Δ</i>	Agglutinin-like sequence protein	[97]	Hyphae	Yes	Yes	Yes	Yes	[94]
<i>pme1Δ/Δ</i>	Mannosyltransferase	[98]	Hyphae	Partial [¶]	Partial [¶]	Partial [¶]	Partial [¶]	[66]
<i>pmt1Δ/Δ</i>	Secretory pathway ATPase	[99]	Hyphae	Partial [¶]	Partial [¶]	Partial [¶]	Partial [¶]	[66]
<i>mnn4Δ/Δ</i>	Regulator of mannosylphosphorylation	[100]	Hyphae	Yes	Yes	Yes	Yes	[66]
<i>mnn9Δ/Δ</i>	Putative mannosyltransferase	[101]	Hyphae	Yes	Yes	Yes	Yes	[66]
<i>mnt1/mnt2Δ/Δ</i>	Mannosyltransferases	[102]	Hyphae	Yes	Yes	Yes	Yes	[66]
<i>chs2/chs3Δ/Δ</i>	Chitin synthase/ Chitin synthase	[103]	Hyphae	Yes	Yes	Yes	Yes	This study
<i>mit1Δ/Δ</i>	Mannose:inositolphosphoceramide mannose transferase	[104]	Hyphae	Yes	Yes	Yes	Yes	[66]
<i>bmt1Δ/Δ</i>	Beta-mannosyltransferase	[105]	Hyphae	Yes	Yes	Yes	Yes	[66]
<i>bmt2Δ/Δ</i>	Putative beta-mannosyltransferase	[105]	Hyphae	Yes	Yes	Yes	Yes	[66]
<i>bmt3Δ/Δ</i>	Beta-mannosyltransferase	[105]	Hyphae	Yes	Yes	Yes	Yes	[66]
<i>bmt4Δ/Δ</i>	Beta-mannosyltransferase	[105]	Hyphae	Yes	Yes	Yes	Yes	[66]
<i>bmt5Δ/Δ</i>	Putative beta-mannosyltransferase	[106]	Hyphae	Yes	Yes	Yes	Yes	[66]
<i>bmt6Δ/Δ</i>	Beta-mannosyltransferase	[106]	Hyphae	Yes	Yes	Yes	Yes	[66]
<i>gsc1Δ/GSCI</i>	Beta-1,3-glucan synthase catalytic subunit	[107]	Hyphae	Yes	Yes	Yes	Yes	[66]
<i>gsl1Δ/Δ</i>	Beta-1,3-glucan synthase subunit	[107]	Hyphae	Yes	Yes	Yes	Yes	[66]
<i>gsl2Δ/Δ</i>	Beta-1,3-glucan synthase subunit	[107]	Hyphae	Yes	Yes	Yes	Yes	[66]
<i>kre6Δ/KRE6</i>	Beta-1,6-glucan synthase subunit	[108]	Hyphae	Yes	Yes	Yes	Yes	This study

[†] Morphology recorded 2 h post-infection on TR146 buccal epithelial cell monolayers; hyphae includes pseudohyphae.

[‡] Data based on Western blotting.

[§] Cytokines includes IL-1 α , IL-6 and G-CSF.

[¶] Damage measured by LDH assay.

^{||} New *ece1Δ/Δ* also created in this study (See Extended Data Table 2). Original mutant (in red) produced by [27] using the URA-blaster protocol [3]. A set of *ece1* mutants, including partial deletion of *ECE1* and a revertant, was produced in this study in the same genetic background using strain BWP17 to avoid a URA3 effect based on genomic location [109, 110].

[¶] Partial activation is due to lack of adhesion.

Extended Data Table 2. *C. albicans* mutant strains constructed and used in this study.

Strain description	Strain name	Genotype
BWP17+Clp30	M1477	<i>ura3::λimm434/ura3::λimm434</i> <i>iro1::λimm434/iro1::λimm434</i> <i>his1::hisG/his1::hisG</i> <i>arg4::hisG/arg4::hisG</i> <i>RPS1/rps1::(URA3-HIS1-ARG4)</i>
<i>ece1Δ/Δ</i>	M2057	<i>ura3::λimm434/ura3::λimm434</i> <i>iro1::λimm434/iro1::λimm434</i> <i>his1::hisG/his1::hisG</i> <i>arg4::hisG/arg4::hisG</i> <i>ece1::HIS1/ece1::ARG4</i> <i>RPS1/rps1::URA3</i>
<i>ece1Δ/Δ+ECE1</i>	M2059	<i>ura3::λimm434/ura3::λimm434</i> <i>iro1::λimm434/iro1::λimm434</i> <i>his1::hisG/his1::hisG</i> <i>arg4::hisG/arg4::hisG</i> <i>ece1::HIS1/ece1::ARG4</i> <i>RPS1/rps1::(URA3-ECE1)</i>
<i>ece1Δ/Δ+ECE1_{Δ184-279}</i>	M2174	<i>ura3::λimm434/ura3::λimm434</i> <i>iro1::λimm434/iro1::λimm434</i> <i>his1::hisG/his1::hisG</i> <i>arg4::hisG/arg4::hisG</i> <i>ece1::HIS1/ece1::ARG4</i> <i>RPS1/rps1::(URA3-ECE1^{Δ184-279})</i>
<i>kex1Δ/Δ</i>	M2258	<i>ura3::λimm434/ura3::λimm434</i> <i>iro1::λimm434/iro1::λimm434</i> <i>his1::hisG/his1::hisG</i> <i>arg4::hisG/arg4::hisG</i> <i>kex1::HIS1/kex1::ARG4</i> <i>RPS1/rps1::URA3</i>
SC5314+p <i>ECE1-GFP</i> (<i>ECE1</i> promoter-GFP)	CA58	<i>ECE1/ece1::GFP-SAT1</i>
BWP17+Clp30+p <i>ENO1-dTom</i> (<i>ENO1</i> promoter-dTom)	RWC83	<i>ura3::λimm434/ura3::λimm434</i> <i>iro1::λimm434/iro1::λimm434</i> <i>his1::hisG/his1::hisG</i> <i>arg4::hisG/arg4::hisG</i> <i>RPS1/rps1::(URA3-HIS1-ARG4)</i> <i>ENO1/eno1::dTom-SAT1</i>
<i>ece1Δ/Δ+pENO1-dTom</i> (<i>ENO1</i> promoter-dTom)	RWC84	<i>ura3::λimm434/ura3::λimm434</i> <i>iro1::λimm434/iro1::λimm434</i> <i>his1::hisG/his1::hisG</i> <i>arg4::hisG/arg4::hisG</i> <i>ece1::HIS1/ece1::ARG4</i> <i>RPS1/rps1::URA3</i> <i>ENO1/eno1::dTom-SAT1</i>
<i>ece1Δ/Δ+ECE1</i> + dTomato	RWC85	<i>ura3::λimm434/ura3::λimm434</i> <i>iro1::λimm434/iro1::λimm434</i> <i>his1::hisG/his1::hisG</i> <i>arg4::hisG/arg4::hisG</i> <i>ece1::HIS1/ece1::ARG4</i> <i>RPS1/rps1::(URA3-ECE1)</i> <i>ENO1/eno1::dTomato-NAT^r</i>
<i>ece1Δ/Δ+ECE1_{Δ184-279}</i> + dTomato	RWC86	<i>ura3::λimm434/ura3::λimm434</i> <i>iro1::λimm434/iro1::λimm434</i> <i>his1::hisG/his1::hisG</i> <i>arg4::hisG/arg4::hisG</i> <i>ece1::HIS1/ece1::ARG4</i> <i>RPS1/rps1::(URA3-ECE1^{Δ184-279})</i> <i>ENO1/eno1::dTomato-NAT^r</i>

Extended Data Table 3. LC-MS/MS analysis of *C. albicans* Ece1-III

Ece1-III sequence	PSM Value* (% total Ece1-III) (% total Ece1p [†])				
	Wild Type	<i>ece1Δ/Δ+ECE1</i>	TR146+Wild type	<i>rEce1p+rKex2p</i>	<i>kex1Δ/Δ</i>
SIIGIIMGILGNIPQVIQIIMSIVKAFKGNK	699 (86%) (41%)	477 (89%) (35%)	79 (97.5%) (97.5%)	n/d [‡]	49 (13.3%) (3.6%)
SIIGIIMGILGNIPQVIQIIMSIVKAFKGNKR	1 (0.1%) (0.06%)	1 (0.2%) (0.07%)	2 (2.5%) (2.5%)	248 (80%) (1.5%)	291 (78.9%) (21%)

*The number of peptide spectrum matches. Data for *ece1Δ/Δ* and *ece1Δ/Δ+ECE1_{del168-179}* are not included as no Ece1-III peptides were detected in either strain, as expected.

[†]% of SIIGIIMGILGNIPQVIQIIMSIVKAFKGNK or SIIGIIMGILGNIPQVIQIIMSIVKAFKGNKR detected amongst all Ece1-III peptides found by LC-MS/MS.

[‡]% of SIIGIIMGILGNIPQVIQIIMSIVKAFKGNK or SIIGIIMGILGNIPQVIQIIMSIVKAFKGNKR detected amongst all Ece1p peptides found by LC-MS/MS.

[§]n/d; not detected.

Extended Data Table 4. Oligonucleotide primers used in this study.

Primer name	Application	Sequence (5'-3')	Description
ECE1-FG	PCR	atcaataaccaccattttcaaaatgtttttttttttatctctacaaca aacacttctctttttactaccaactttttccattgtaaagaagcttc gtacgctgcaggtc	Construction of <i>ECE1</i> deletion construct
ECE1-RG	PCR	cacaaaaacaacaataaaaaaatcagttacagcaaaagtgcacaag acttatggataaaagattaaactgtgggaaacaaattttctgctgag cattctgatcatcgatgaattcgag	Construction of <i>ECE1</i> deletion construct
ECE1-RecF3k	PCR	gcacgctctaaagtggagtaacaac	Construction of <i>ECE1</i> complementation plasmid
ECE1-RecR	PCR	ggtcgacccagacgttggtgc	Construction of <i>ECE1</i> complementation plasmid
ECE1-F1	PCR	ggcttctcataaatgaaggctcag	Confirmation of <i>ECE1</i> deletion
ECE1-R1	PCR	gccaatcaatcttctgctgccac	Confirmation of <i>ECE1</i> deletion
KEX1-FG	PCR	tatctttttttttttttaccctctcatcttacaacctgtacactt acctaacaacacacactctctttaaatacaacacaaatcaattgaa gcttctgacgctgcaggtc	Construction of <i>KEX1</i> deletion construct
KEX1-RG	PCR	tcacaatctagattattgtaggtgtatagacaaaaataaaatcaaac attattcgttataaaactacaagatcttaactctcactgtaccgaaaaat tctgatcatcgatgaattcgag	Construction of <i>KEX1</i> deletion construct
KEX1-F1	PCR	ggaaagccataagaattgga	Confirmation of <i>KEX1</i> deletion
KEX1-R1	PCR	aggaaagctgtggtgtagtg	Confirmation of <i>KEX1</i> deletion
HIS-F2	PCR	ggacgaattgaagaagctggtcaaccg	Confirmation of <i>ECE1/KEX1</i> deletion
HIS-R2	PCR	caacgaaatggcctccctaccacag	Confirmation of <i>ECE1/KEX1</i> deletion
ARG-F2	PCR	ggatatgttgctactgatttag	Confirmation of <i>ECE1/KEX1</i> deletion
ARG-R2	PCR	aatggatcagtgaccggctg	Confirmation of <i>ECE1/KEX1</i> deletion
ECE1-Fint1	PCR	ctaactgtttgatggcctctg	Confirmation of plasmid integration
URAF2	PCR	ggagttggattagatgataaagtgatgg	Confirmation of plasmid integration
RPF-1	PCR	gagcaggtacacacacacacttg	Confirmation of plasmid integration
RPF-2	PCR	cgccaaagagttcccctattatc	Confirmation of plasmid integration
Pep3-F1	PCR	gaagatcgcattctgttctgctgg	Excision of Ece1-III ₆₂₋₉₃ from <i>ECE1</i>
Pep3-R1	PCR	cagaatcgatctctcttttgtaatagcagattgaattcttg	Excision of Ece1-III ₆₂₋₉₃ from <i>ECE1</i>
5'ECE1prom-NarI	PCR	gatcggcgctccagccactattttgtacctgt	Amplification of <i>ECE1</i> promoter region for <i>ECE1</i> promoter-GFP construct
3'ECE1prom-XhoI	PCR	tcagctcaggttaacgaatggaaaatagttggtag	Amplification of <i>ECE1</i> promoter region for <i>ECE1</i> promoter-GFP construct
5'ECE1term-SacII	PCR	gatcccgcggcagcagataaaaattgtttccacaag	Amplification of <i>ECE1</i> terminator region for <i>ECE1</i> promoter-GFP construct
5'ECE1term-SacI	PCR	tcaggagctccgtaagaatgaatgacagttggtgc	Amplification of <i>ECE1</i> terminator region for <i>ECE1</i> promoter-GFP construct
G1-ECE1	PCR	ctcgtctagtagttcaagagt	Confirmation of <i>ECE1</i> -GFP plasmid integration (5' end)
GFP veri rev	PCR	tgatctgggtatctcgaagcat	Confirmation of <i>ECE1</i> -GFP plasmid integration (5' end)
G4-ECE1	PCR	tggaaagattcacttgatggaac	Confirmation of <i>ECE1</i> -GFP plasmid integration (3' end)
X3-SAT1	PCR	gtgaagtgtgaaggaggag	Confirmation of <i>ECE1</i> -GFP plasmid integration (3' end)
pENO1 FW	PCR	tccttggctggcactgaactcg	Confirmation of pENO1-dTom plasmid integration
dTom REV	PCR	aaggtctactctcacctcacc	Confirmation of pENO1-dTom plasmid integration
ACT1-F	qPCR	tcagaccagctgatttagtttg	Quantification of actin cDNA
ACT1-R	qPCR	gtgaacaatggatggaccag	Quantification of actin cDNA
ECE1-F	qPCR	atcgaatccaagagag	Quantification of <i>ECE1</i> cDNA
ECE1-R	qPCR	agcatttcaatccgacag	Quantification of <i>ECE1</i> cDNA